

Morphology of Single Olivocerebellar Axons Labeled With Biotinylated Dextran Amine in the Rat

I. SUGIHARA, H.-S. WU, AND Y. SHINODA*

Department of Physiology, Tokyo Medical and Dental University School of Medicine,
1–5–45 Yushima, Bunkyo-ku, Tokyo 113–8519, Japan

ABSTRACT

The morphology of olivocerebellar (OC) axons originating from the inferior olive (IO) was investigated in the rat by reconstructing the entire trajectories of single axons that had been labeled with biotinylated dextran amine. Virtually all of the OC axons entered the cerebellum through the inferior cerebellar peduncle (ICP) contralateral to the IO, with a few exceptions. Although most OC projection was contralateral, a few axons projected bilaterally by crossing the midline within the cerebellum. Collaterals of OC axons could be classified into thick branches and thin collaterals. Thick branches of each OC axon (6.1 ± 3.7 /OC axon, mean \pm SD for $n = 16$ axons) terminated as climbing fibers (CFs) on single Purkinje cells (PCs) in a one-to-one relationship. Besides terminal arborization around PC thick dendrites, CFs had terminals that surrounded a PC soma, fine branchlets that extended transversely in the molecular layer, and thin retrograde collaterals that re-entered the PC and granular layers. Innervation of a single PC by two CFs originating from the same axon was seen, although infrequently. Concerning thin collaterals, about half of the OC axons had one or only a few collaterals terminating in the white matter of the ICP, most had 1 to 6 collaterals terminating in a single cerebellar nucleus, and all had 3 to 16 collaterals that terminated mainly in the granular layer, but occasionally in the cerebellar white matter and the PC layer. Some swellings of thin collaterals touched somata of presumed Golgi cells and PCs. No OC axons terminated solely in the ICP, cerebellar nucleus or granular layer without giving rise to CFs. *J. Comp. Neurol.* 414:131–148, 1999. © 1999 Wiley-Liss, Inc.

Indexing terms: afferent pathways; cerebellar cortex; cerebellar nuclei; nerve endings; medulla oblongata; Purkinje cells

Since the discovery of climbing fibers (CFs) in the cerebellar cortex (Ramón y Cajal, 1911), the morphology of these fibers has been extensively studied by Golgi staining (Ramón y Cajal, 1911; Scheibel and Scheibel, 1954; Fox et al., 1969), electron-microscopy (Hámori and Szentágothai, 1966; Palay and Chan-Palay, 1974), and recently anterograde labeling (Van der Want et al., 1989; Rossi et al., 1991; Sugihara et al., 1996). These studies have revealed the details of the local morphology of CFs, including strong synaptic contacts with thick dendrites of Purkinje cells (PCs), branching in the granular layer, and collateral termination on Golgi cells and cerebellar nucleus neurons.

It has been established electrophysiologically (Eccles et al., 1966a) and anatomically with degeneration methods (Szentágothai and Rajkovits, 1959; Desclin, 1974) that neurons in the inferior olive (IO) are the origin of CFs. The final portion of an olivocerebellar (OC) axon in the cerebellar cortex takes the form of a CF. OC projection has been shown to have a special topography that divides the

cerebellar cortex into several longitudinal compartments (Groenewegen and Voogd, 1977; Oscarsson and Sjölund, 1977; Voogd and Bigaré, 1980; Wiklund et al., 1984; Buisseret-Delmas and Angaut, 1993).

Despite abundant anatomic and physiological studies on the OC system, there is little information available on the organization of OC projection at the level of single axons. For example, the exact number of CFs that a single OC axon gives rise to is not known, although the average number of CFs per OC axon (about seven in the rat) was inferred by counting the total numbers of PCs and IO

Grant sponsor: CREST (Core Research for Evolutional Science and Technology) of the Japan Science and Technology Corporation; Grant sponsor: Ministry of Education, Science, and Culture of Japan.

*Correspondence to: Yoshikazu Shinoda, Department of Physiology, Tokyo Medical and Dental University, School of Medicine, 1–5–45 Yushima, Bunkyo-ku, Tokyo 113–8519, Japan. E-mail: yshinoda.phy1@med.tmd.ac.jp

Received 1 March 1999; Revised 8 July 1999; Accepted 20 July 1999

neurons (Schild, 1970). Electrophysiological studies (Faber and Murphy, 1969; Armstrong et al., 1973; Ekerot and Larson, 1982) and retrograde labeling studies (Brodal et al., 1980; Rosina and Provini, 1983; Wiklund et al., 1984; Hrycyszyn et al., 1989) have shown that single OC axons project to separate sites in the cerebellar cortex, but the general extent of the spread of single OC axons in the cerebellar cortex remains unknown. One-to-one innervation of a CF to a target PC has been suggested anatomically (Ramón y Cajal, 1911) and demonstrated electrophysiologically (Eccles et al., 1966a). However, multiple innervation occurs in young animals and several kinds of adult animals that have an abnormal granule cell-parallel fiber system (Crepel et al., 1976; Mariani, 1983). Even in adult animals, the presence of multiple innervation by "retrograde collaterals" of CFs has been suggested (Scheibel and Scheibel, 1954). In this regard, it would be worth re-examining morphologically the prevalence of one-to-one innervation of PCs by CFs in normal adult animals. Non-CF thin collaterals of OC axons innervate Golgi cells in the granular layer (Hámori and Szentágothai, 1966; Fox et al., 1969; Chan-Palay and Palay, 1971) and cerebellar nucleus neurons (Van der Want et al., 1989; Sugihara et al., 1996). However, the number, targets, and morphology of non-CF collaterals of OC axons have not been fully clarified. An analysis of the entire trajectories of single OC axons should answer some of these fundamental questions on the organization of OC projection.

Intra-axonal staining with horseradish peroxidase of electrophysiologically identified neurons has been successfully used by our group to analyze the trajectories of single axons of various neurons (Futami et al., 1979; Shinoda et al., 1981, 1986, 1992). With this method, we have revealed the detailed morphology of single mossy fibers in the cerebellar cortex (Krieger et al., 1985) and the cerebellar nuclei (Shinoda et al., 1992). However, this method has not been useful for staining single OC axons, because even their stem axons are too thin to be penetrated under good conditions. As anterograde tracers, biotinylated dextran amine (Veenman et al., 1992; Sugihara et al., 1996), and *Phaseolus vulgaris* leucoagglutinin (Van der Want et al., 1989; Kakei and Shinoda, 1990; Rossi et al., 1991; Sugihara et al., 1993) have made it possible to trace the precise trajectories of single axons. These tracers have been applied in studies on OC projection within localized areas in the cerebellar cortex and the cerebellar nuclei (Van der Want et al., 1989; Rossi et al., 1991; Sugihara et al., 1993, 1996).

The purpose of the present study was to analyze the entire trajectories of single OC axons that had been labeled by the injection of biotinylated dextran amine into the IO in the rat. By reconstructing entire axons on serial sections, we examined the detailed morphologic characteristics of single OC axons, i.e., their paths in the medulla and cerebellum, the laterality of projection, ramification patterns, CF and non-CF terminations in the cerebellar cortex and cerebellar nuclei, and innervation patterns of CFs with regard to a PC.

MATERIALS AND METHODS

Twenty-three Long-Evans rats of both sexes were used in these experiments. The rats weighed 230–350 g and were 3–5 months old. The surgery and animal care conformed to "The Principles of Laboratory Animal Care"

(NIH publication No. 85–23, revised in 1985) and "Guiding Principles for the Care and Use of Animals in the Field of Physiological Sciences" (The Physiological Society of Japan, 1988), and the experimental protocol was confirmed by Animal Care and Use Committee in Tokyo Medical and Dental University.

Surgical procedures and tracer application

The animals were anesthetized with an intraperitoneal injection of ketamine (130 mg/kg body weight) and xylazine (Rompun, Bayer, Germany; 8 mg/kg). Atropine (0.4 mg/kg) was also given intraperitoneally. They were then placed in a stereotaxic apparatus in a supine position. Heart rate and rectal temperature were monitored continuously. Supplemental doses of ketamine (13 mg/kg) and xylazine (1 mg/kg) were given every 30 minutes starting 1 hour after the initial dose, as required. A heating pad was used to keep the rectal temperature between 35 and 37°C. After incision of the neck skin, the trachea and esophagus together with the musculature around them were pulled aside to expose the base of the cranium. A hole was drilled in the bone, and a cut was made in the dura. The basilar artery and its bifurcation were used as landmarks to locate the IO. In four animals, the IO was approached from the dorsal side near the obex. In these cases, the animal was put on the stereotaxic apparatus normally with the head tilted 45 degrees nose-down, and a cut was made in the ligament between the skull and the first vertebra.

An anterograde tracer, biotinylated dextran amine (D-1956, 10,000 MW, Molecular Probes, Eugene, OR) was dissolved in physiological saline to give a concentration of 10–15%. A glass micropipette (tip diameter, 4 µm) was filled with this solution and inserted into the IO. Neural activities were recorded from the pipette to locate the IO by its synchronous and rhythmical spontaneous activity (Sugihara et al., 1995; Lang et al., 1996). A very small volume was injected either with pressure (0.001–0.05 µl) or electrophoresis (2 µA positive current pulses of 1-second duration at 0.5 Hz for 5–20 minutes). Pipettes were left in situ for 5 minutes after injection before they were withdrawn. The wound was cleaned with povidone-iodine, and an antibiotic (cefmetazole) was applied to the wound before suturing.

Besides the injection of small amounts of tracer in the IO as described above (n = 15), a larger volume of biotinylated dextran amine was also injected into the IO (n = 4, 0.1–0.2 µl) to label a larger number of OC axons, into the cerebellar nucleus to label PCs retrogradely (n = 2, 0.1 µl) and into the lateral medulla to label IO neurons retrogradely (n = 2, 4 µl). The histologic procedures for these experiments were the same as for the above experiments.

Fixation and histochemistry

After a survival period of 4 to 7 days, the animals were deeply anesthetized with ketamine (150 mg/kg) and xylazine (12 mg/kg), and perfused through the ascending aorta. Chilled perfusate containing 0.8% NaCl, 0.8% sucrose, and 0.4% glucose in 0.05 M phosphate buffer (pH 7.4, about 4°C, and about 400 ml) was given, and followed by fixative containing 2% paraformaldehyde, 0.6% glutaraldehyde, and 4% sucrose in 0.05 M sodium phosphate buffer (pH 7.4, about 4°C, and about 500 ml). Dissected brains (cerebellum and medulla oblongata) were kept in the same fixative overnight at 4°C and then in 30% sucrose in phosphate

buffer (0.05 M, pH 7.4, 4°C) for 1–2 days. The brain was then embedded in a gelatin block.

Serial coronal or parasagittal sections 50 μm thick were cut on a freezing microtome. Sections were treated with biotinylated peroxidase-avidin complex (Standard ABC kit KT-4000, Vector, Burlingame, CA), and a cobalt-glucose oxidase method (Itoh et al., 1979; Van der Want et al., 1989; Rossi et al., 1991) was used for the diaminobenzidine reaction. The sections were then mounted on chrome alum-gelatinized slides, dried overnight, and cover-slipped with Permount. Some sections were counterstained with thionine.

Light microscopic reconstruction

Drawings of labeled axons were made at an objective magnification of $\times 20$ to $\times 100$, with the aid of a Nikon microscope or a three-dimensional imaging microscope (R400; Edge Scientific Instrument, Santa Monica, CA) equipped with a camera lucida apparatus. The later microscope enabled three-dimensional views of the object, as a low-power stereomicroscopes, under any magnifications by using multiple light sources with polarizing filters and eyepieces with polarizing filters. Trajectories of single-labeled OC axons were reconstructed on serial sections by connecting properly cut ends of an axon on one section to the corresponding cut ends of the same axon on the successive sections, as was done with the intra-axonal injection of horseradish peroxidase (Futami et al., 1979; Shinoda et al., 1981, 1986, 1992). Reconstructions in the sectioning plane (coronal or parasagittal) were sometimes converted to those in other planes (parasagittal, coronal, or horizontal).

In drawings of camera lucida images, fibers and swellings were drawn thicker than scale for clarity, as is conventionally done in drawings of reconstructed fibers. The cerebellar lobules were defined according to Larsell (1952) and Voogd (1995). Cerebellar zones of OC projection were defined according to Buisseret-Delmas and Angaut (1993), Voogd (1995), and Voogd et al. (1996). The cerebellar white matter was arbitrarily classified into three parts to aid in describing branching locations. Deep cerebellar white matter meant the white matter excluding the folial white matter, and proximal and distal folial white matter meant the white matter in the deep and apical halves of each folium, respectively.

RESULTS

Single axons were reconstructed in 11 animals in which a small number of axons were well labeled. Spread of the tracer was localized within the IO and ranged from approximately 0.1 to 0.2 mm in diameter in these animals (Fig. 1). Labeled terminal arborizations of CFs were seen in the molecular layer of localized areas of the cerebellar cortex, and no mossy fiber rosettes were seen in any part of the cerebellar cortex in these animals. All axons labeled well enough to be reconstructed passed through the inferior cerebellar peduncle (ICP) contralateral to the injection site, but no or a few very faintly labeled axons were seen in the ipsilateral ICP in each animal. Sixteen axons terminating in the vermis (lobules VI, VII, VIII, and IX), intermediate area (lobule III, simple, ansiform, and paramedian lobules), hemisphere (ansiform lobule and copula pyramidis), and flocculus were reconstructed in these animals. In eight of them, the entire trajectories of single OC axons

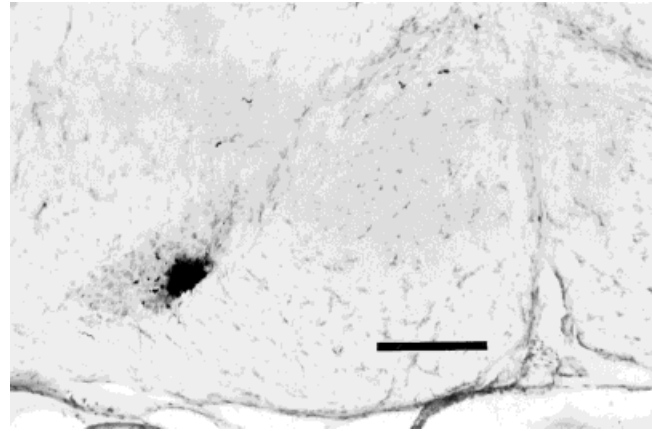


Fig. 1. Photomicrograph of a coronal section including an injection site in the left caudal medial accessory olive. Scale bar = 200 μm .

could be traced. In the other eight axons, all thick branches terminating as CFs were completely reconstructed, but a few thin collaterals, which presumably terminated in the granular layer (see later section), could not be traced completely, because they were intermingled with other labeled axons. Stem axons of these 16 reconstructed axons were traced down to the injection site in the IO, although their cell bodies were not identified. Besides these axons, 46 partially reconstructed axons, which were identified as OC axons because of the injection site in the IO and at least one reconstructed CF, was used to supplement the data.

Pathway of OC axons in the brainstem

Twenty-one OC axons (including the 16 OC axons that were completely reconstructed) were reconstructed in the brainstem as far as their individual injection sites, and the trajectories of 11 of them are shown in Figure 2A–C. Axons left an injection site toward the contralateral side, crossed the midline, ran transversely above or through the contralateral IO, and entered the white matter of the ICP between the lateral surface of the medulla and the spinal trigeminal tract. They then ran dorsally and slightly rostrally through the ICP under the lateral surface of the medulla into the dorsolateral part of the ICP. There they changed directions and ran longitudinally through the dorsolateral ICP (arrows in Fig. 2A–D) to enter the cerebellum. They did not ramify in the brainstem, except for thin collaterals in the ICP near the junction to the cerebellum (see later sections). All of the labeled OC axons formed a relatively localized and delineated bundle in the ICP contralateral to the injection site in each experiment.

There seemed to be a rostrocaudal arrangement among OC axons in the ventrolateral and lateral part of the ICP (Fig. 2B,C), which corresponded to the relative rostrocaudal locations of OC neurons in the IO. Axons terminating in the vermis ran through the very rostral portion of the ICP, which was located above the superior cerebellar peduncle and the parabrachial nucleus, and beneath the dorsal surface of the pons. They made a U-shaped turn there (Fig. 2A–D, filled arrowheads) and then ran caudo-medio-dorsally to enter the cerebellar white matter rostral to the fastigial nucleus. On the other hand, axons projecting to the hemisphere or the intermediate area ran through

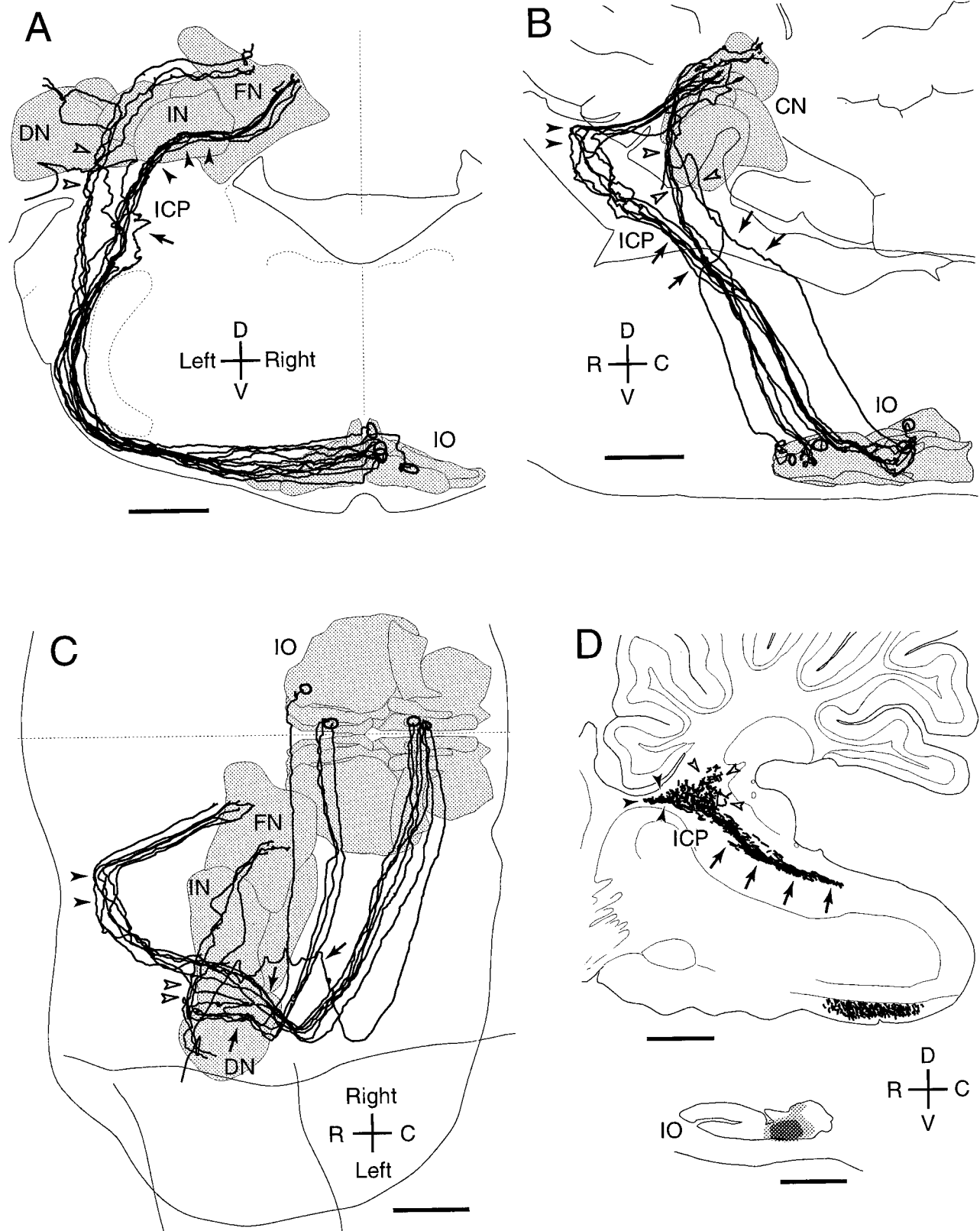


Fig. 2. Paths of reconstructed olivocerebellar (OC) axons in the brainstem. **A–C:** Trajectories in coronal (A), sagittal (B), and horizontal (C) planes of 11 axons reconstructed from 37–93 sections in four experiments. Contours of subdivisions of the inferior olive (IO) and cerebellar nuclei (gray) and the outline of the brain are shown. Thin collaterals are not shown here. Circles in the IO indicate injection sites. **D:** A camera lucida drawing of labeled OC axons in a parasagittal section, including the inferior cerebellar peduncle (ICP). Filled and open arrowheads indicate axons passing through the rostral and

caudal ICP, respectively, and arrows indicate axons running through the dorsolateral part of the ICP in A–D. See text for details. Inset, injection site in this experiment. The volume of tracer injected was large and covered the portion from the central to the caudal medial accessory olive. CN, cerebellar nuclei; ICP, inferior cerebellar peduncle; IN, interposed cerebellar nucleus; IO, inferior olive; DN, dentate nucleus; FN, fastigial nucleus; D, dorsal; V, ventral; R, rostral; and C, caudal. Scale bars = 1 mm.

the caudal portion of the ICP at the junction to the cerebellum (Fig. 2A–D, open arrowheads). In a preparation in which many axons terminating in the vermis and hemisphere were simultaneously labeled by injecting a relatively large volume of tracer into the region from the central to the caudal medial accessory olive of the IO, continuous occupation of the labeled axons from the rostral to the caudal ICP at the junction to the cerebellum was observed (Fig. 2D, filled and open arrowheads), indicating that these pathways were not completely separate. Further detailed analysis of the axonal paths in the ICP indicated that axons terminating in vermal zone A (Buisseret-Delmas and Angaut, 1993; Voogd, 1995; Voogd et al., 1996) ran through a rostral portion, axons terminating in zone B or lateral zone A ran through either a rostral, caudal, or intermediate portion, and axons terminating in zone C2 or D or the flocculus ran through a caudal portion of the ICP at the junction to the cerebellum.

Laterality of OC axons in the ICP with regard to their origin in the IO

To examine whether all OC axons pass through the contralateral ICP, a large volume of tracer was injected into the ICP in the medulla in two animals. Most of the neurons in the contralateral IO were retrogradely labeled (Fig. 3A). Much fewer neurons were labeled ipsilaterally in the ventral medulla, and most of them were outside of the contour of the IO and differed with regard to shape and size from round or polygonal small IO neurons. However, seven and nine labeled neurons in each animal, respectively, were seen in the medial portion of the ipsilateral dorsomedial cell column subnucleus (DMCC) of the IO in these experiments (Fig. 3B, arrowheads). Because these neurons were similar in size and shape to labeled olivary neurons on the contralateral side and the bilateral DMCCs are continuous across the midline (de Zeeuw et al., 1996), these ipsilateral neurons were likely to be olivary neurons. Except for these neurons in the DMCC, two and three labeled small round cells were seen in the ipsilateral IO, but we could not identify them as IO neurons, because their locations were not consistent in the two animals. Therefore, we concluded that virtually all of the IO neurons except for some in the medial DMCC project to the cerebellum through the contralateral ICP.

Axonal pathway and ramification in the cerebellar white matter

Axons that passed through the rostral ICP entered the deep cerebellar white matter rostral to the fastigial nucleus, whereas those that passed through the caudal ICP entered the cerebellar white matter rostral to the dentate nucleus (Fig. 2C, filled and open arrowheads). Among the latter axons, those innervating the intermediate area or medial hemisphere ran medially through the white matter rostral or dorsal to the cerebellar nuclei. Axons innervating the flocculus entered the floccular stalk rather directly from underneath the dentate nucleus (a case is shown in Fig. 2, and also see Fig. 12A).

After entering the cerebellum, stem axons frequently ramified into many branches in the deep cerebellar white matter (Fig. 4). These ramifications often occurred when the stem axons reached the semi-parasagittal plane in which branches terminated as CFs, as suggested in a mass labeling study (Van der Want et al., 1989). However, exceptions were occasionally seen. In the axon shown in

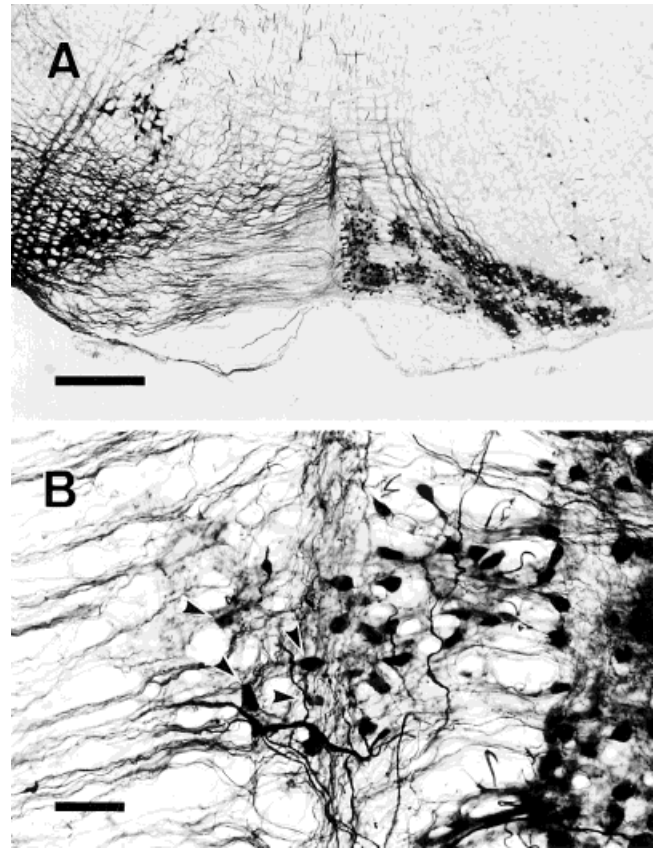


Fig. 3. Retrograde labeling of inferior olive (IO) neurons by injecting a large volume of biotinylated dextran amine in the left lateral medulla. **A:** Coronal section showing the IO. **B:** Magnified photomicrograph showing the bilateral dorsomedial cell column subnuclei (DMCCs). The sections were weakly counterstained. Arrowheads indicate labeled neurons in the DMCC ipsilateral to the injection site. Scale bars = 500 μ m in A; 100 μ m in B.

Figure 4A, a branch that terminated in the right lobule IX and the posterior interposed cerebellar nucleus was given off at a position (arrow) more lateral than the other branches. Stem axons and branches usually ran in the white matter rostral and dorsal to the cerebellar nuclei, but sometimes they ran through or beneath the cerebellar nuclei. Branches entered the folial white matter, ramified, and ran along each other in the semi-parasagittal plane to reach the areas for their termination in the cerebellar cortex, in which they further ramified. The branches ran, more or less, along the longitudinal axis of a folium in the folial white matter, but hairpin-shaped returning was sometimes encountered (see arrow in Fig. 12A).

The diameters of the branches were not even (Fig. 5A–C), as in a completely reconstructed OC axon (Fig. 5D,F), in which the diameters of branches were measured just after each branching point in the cerebellar white matter and in the ICP (Fig. 5E). The branches of OC axons were grouped into thick branches (0.7–1.4 μ m in diameter) and thin collaterals (0.2–0.5 μ m in diameter; see below). The diameter of stem axons was within the range of that of thick branches. The diameters of thick branches did not seem to decrease significantly after repeated branching into daughter thick branches. Once a thick branch entered the granular layer, it took a straight or winding course

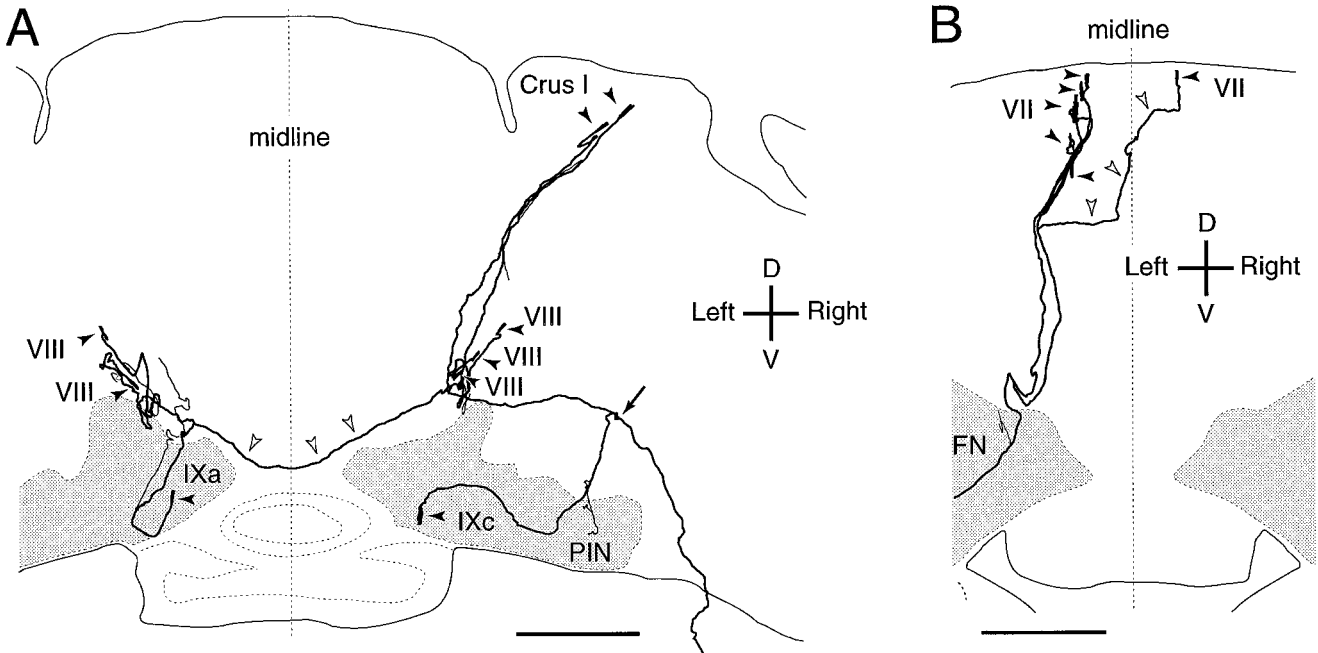


Fig. 4. **A,B:** Frontal view of the trajectories of two reconstructed olivocerebellar axons that had bilateral projections. Filled arrowheads indicate climbing fibers (CFs) terminal arborizations, and open arrowheads indicate axons crossing the midline. Vertical dotted lines indicate the midline. The lobule in which each CF terminated is

indicated in Roman letters. The arrow in A indicates the first bifurcation of a stem axon into thick branches. Thin collaterals terminating in the cerebellar cortex are not shown in B. PIN, posterior interposed cerebellar nucleus; FN, fastigial nucleus; D, dorsal; V, ventral. Scale bars = 1 mm.

toward the PC layer for a distance of usually less than several hundred micrometers and terminated as a CF on a single PC.

The occurrence of the ramification of thick branches in the deep white matter, proximal and distal folial white matter, and granular layer was 37 (46%), 23 (28%), 15 (19%), and 6 (7%), respectively, in 16 reconstructed OC axons (81 branching points). Thus, ramifications were most frequent in the deep cerebellar white matter and the proximal folial white matter. A single OC axon generated 2–17 final thick branches (6.1 ± 3.7 , mean \pm SD, $n = 16$), each of which innervated a PC as a CF.

Laterality of OC projection within the cerebellum

Most of the reconstructed OC axons terminated on the side contralateral to the IO from which they originated. However, some OC axons terminated in the ipsilateral cerebellar cortex and in the contralateral cerebellar cortex. In the example shown in Figure 4A, a stem axon entered the cerebellum through the ICP contralateral to its origin in the IO and sent several branches to the contralateral posterior interposed cerebellar nucleus and cerebellar cortex. A thick branch of this OC axon crossed the midline in the deep cerebellar white matter (Fig. 4A, open arrowheads) and gave rise to three CFs and some thin collaterals in the ipsilateral cerebellum. These CFs were located contralaterally in crus I, bilaterally in lobule VIII in the medial hemisphere, and lobule IX in the lateral vermis (Fig. 4A, filled arrowheads). The projection area of this axon seemed to be in zone C2, because a collateral innervated the posterior interposed cerebellar nucleus, and the cortical termination area was in the medial hemisphere and lateral vermal lobule IX (Voogd, 1995). The other

example in Figure 4B shows an OC axon that originated from the caudal medial accessory olive and terminated in lobule VII with a nuclear collateral in the contralateral fastigial nucleus. This topographical relationship indicated that the cortical projection area of this axon was in vermal zone A. One of the branches of this axon crossed the midline within the folial white matter (Fig. 4B, open arrowheads) and formed a single CF that terminated near the apex of lobule VII ipsilateral to the IO from which the axon originated. The termination areas of the ipsilateral and contralateral CFs were nearly symmetrical to the midline in these two axons (Fig. 4A,B, filled arrowheads).

The frequency of transcerebellar ipsilateral projection was estimated from 11 experiments in which a small volume of tracer was injected into the IO (excluding the DMCC) and no labeled axons were seen to enter the cerebellum through the ipsilateral ICP. Ipsilateral projection was found in two of the 11 experiments. The total number of labeled axons crossing the midline in the cerebellum versus the total number of labeled stem axons counted in the ICP in these experiments was 4 to 115 (about 3%). This indicated that ipsilateral projection, though present, was very weak. The existence of axons that terminate exclusively on the ipsilateral side by intracerebellar crossing was not determined.

Terminal arborization of CFs

The most distal thick branch of an OC axon, which was equivalent to a CF, reached a target PC at its soma (Fig. 6A,C,E) or occasionally at its main thick dendrite (Fig. 6D) through the granular (Fig. 6A,D,E) or PC layers (Fig. 6C). The CF then ran along the surface of the thick dendrite toward its distal portion as a main stalk fiber of a terminal

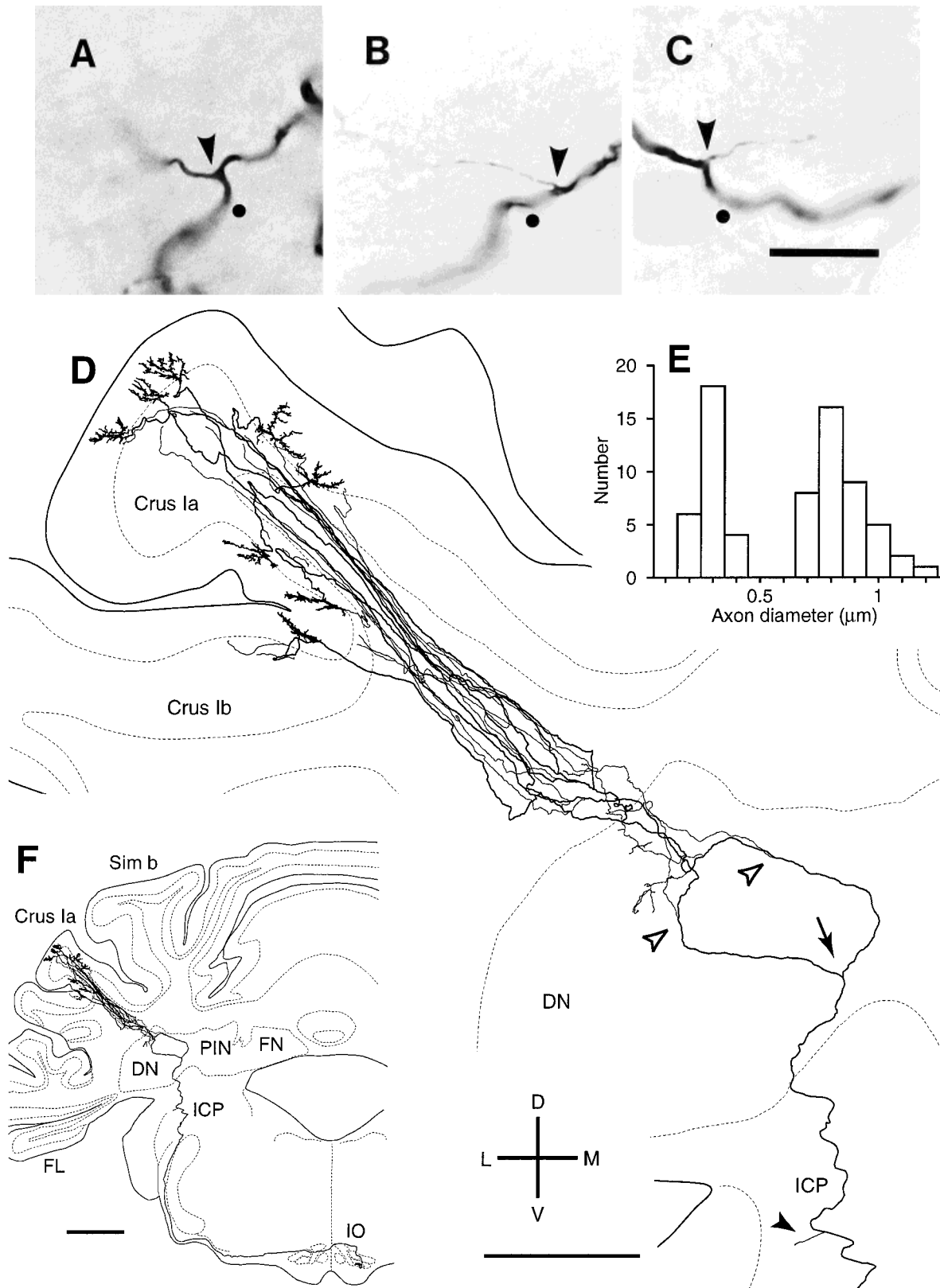


Fig. 5. Thick branches and thin collaterals of an olivocerebellar (OC) axon. **A**: Photomicrograph of a bifurcation into two thick branches. **B**: Bifurcation into a thick branch and a thin collateral. **C**: Bifurcation into a thick branch and a thin collateral terminating in the inferior cerebellar peduncle (ICP). Arrowheads indicate branching points. Circles indicate stem fibers. **D**: Frontal view of the trajectory of a single OC axon innervating crus Ia, reconstructed from 32 serial coronal sections. Biotinylated dextran amine was injected into the dorsal lamella of the principal olive. The origin (dorsal lamella of the principal olive) and termination (lateral hemisphere and the dorsal portion of the dentate nucleus) of this axon indicated that it belonged to zone D1 (Buisseret-Delmas and Angaut, 1993; Voogd, 1995). Filled

arrowhead indicates a thin collateral in the ICP, an arrow indicates the first bifurcation into two thick branches, and open arrowheads indicate the first two branching points of thin collaterals that terminated in the granular layer. **E**: Distribution of diameters of branches measured at 35 branching points of the same axon as in D that occurred in the white matter and the granular layer. See text for details. **F**: Entire trajectory of this axon. ICP, inferior cerebellar peduncle; DN, dentate nucleus; FN, fastigial nucleus; PIN, posterior interposed cerebellar nucleus; Sim b, sublobule b of the simple lobule; FL, flocculus; D, dorsal; V, ventral; L, lateral; M, medial. Scale bars = 10 μ m in A-C; 0.5 mm in D; 1 mm in F.

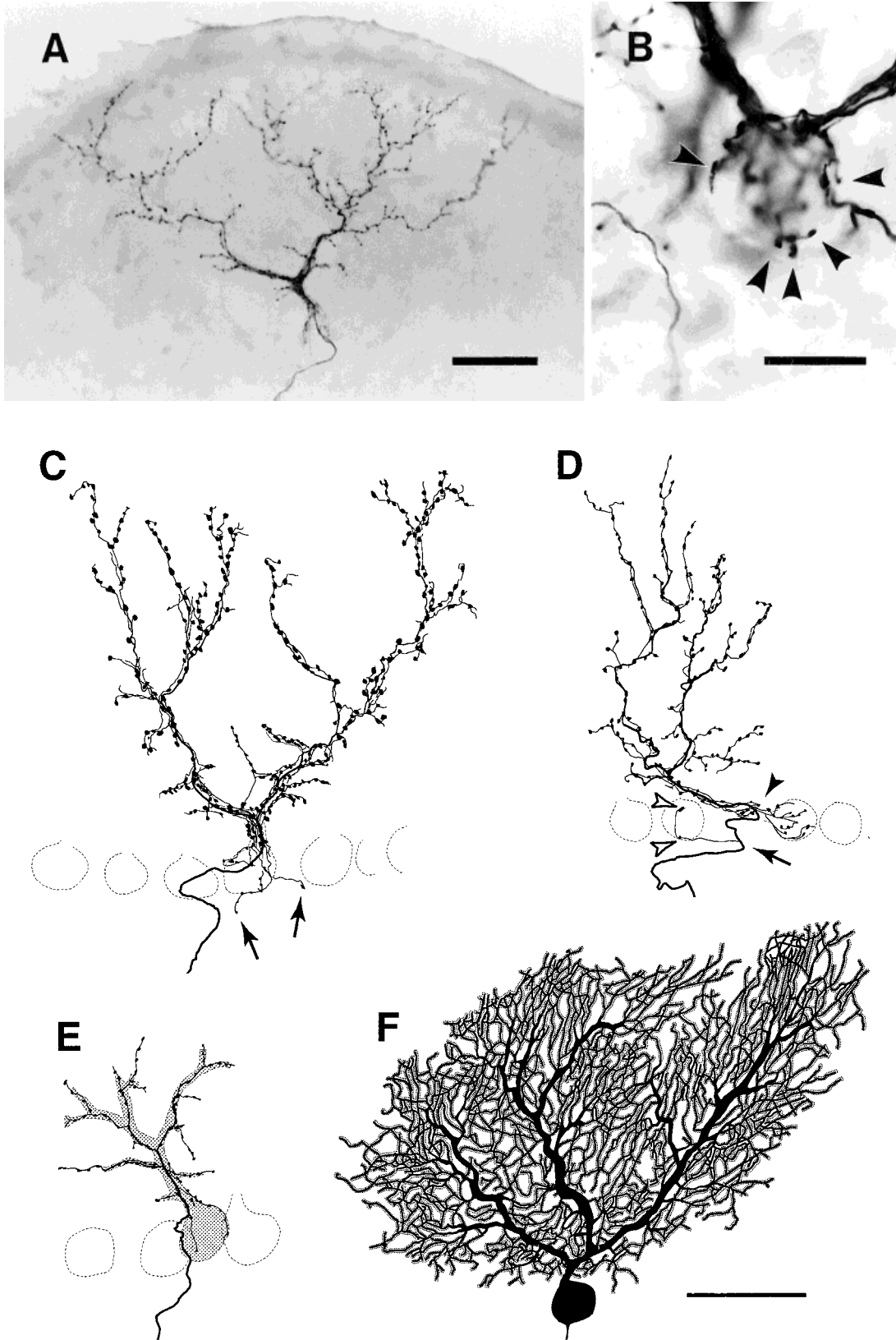


Fig. 6. Terminal arborizations of labeled climbing fibers (CFs) in parasagittal sections. **A:** Photomicrograph of a CF terminal arborization (lobule IX). **B:** Photomicrograph of tendril fibers and swellings (arrowheads) that surrounded the soma of a target Purkinje cell (PC). **C:** Reconstruction of a terminal arborization from two sections (vermal lobule VIa). Arrows indicate retrograde collaterals. **D:** Reconstruction of a terminal arborization from two sections. This CF first reached the dendrite (filled arrowhead) of a PC. A thin collateral terminating in the PC layer (open arrowheads) was given off from this CF (arrow).

E: Camera lucida drawing of a CF and a target PC labeled simultaneously. This PC was faintly labeled by background reaction or the transsynaptic uptake of biotinylated dextran amine. Labeling of this CF was weaker than that in A–D. **F:** Reconstruction of a PC labeled for comparison from two sections. This cell was labeled retrogradely with the injection of biotinylated dextran amine into the fastigial nucleus. The surface of the cerebellar cortex is to the top in each panel. Scale bars = 50 μ m in A; 20 μ m in B; 50 μ m in F (applies to C–F).

arborization. Together with the ramification of thick dendrites, the main stalk fiber ramified into branches of stalk fibers, which ran along individual branches of the thick dendrites. The stalk fibers around PC dendrites gave rise to many thin fibers (diameter, about 0.2–0.3 μm), which generally ran in parallel with stalk fibers, but sometimes ran crossways to surround a PC dendrite like a net (Fig. 6B,C), which is consistent with the definition of a “tendrill” (Palay and Chan-Palay, 1974; Ito, 1984). Tendril fibers bore frequent en passant and terminal swellings. The number of tendrill fibers surrounding a main thick dendrite was five to eight. The stalk fibers in this area were still thick (diameter, about 1 μm) and generally smooth. At more distal portions of the thick dendrites, the number of tendrill fibers decreased, the stalk fibers became thinner, and bore many en passant swellings. It seemed that stalk and tendrill fibers did not innervate distal dendrites characterized by the presence of spines visible under a light microscope (Fig. 6F). The number of swellings on the terminal arborization of a single CF was 154–321 (249.8 ± 42.2 , $n = 32$ terminal arborizations). The diameter of swellings ranged from 0.5 to 2.0 μm , mostly 1.2–1.6 μm . Assuming 6.1 CFs per OC axon (see earlier section), 249.8 swellings per CF corresponded to 1,524 swellings on CF terminal arborizations per OC axon, on average.

In a few preparations, some PCs were faintly labeled, presumably due to either background reaction or to the transsynaptic transfer of the tracer. When labeling of a CF was not too strong to conceal PC labeling, it was possible to see both the CF and the PC clearly. We found 12 pairs of the simultaneous labeling of a CF and its innervated PC (Fig. 6E). A terminal arborization of a CF covered all of the thick dendrites of the target PC in all cases.

Previous studies have noted very weak or absent innervation of a PC soma by a CF (Ramón y Cajal, 1911; Fox et al., 1969; Palay and Chan-Palay, 1974). However, in the present study, 5 to 10 tendrill fibers extended down from a terminal arborization around a PC main dendrite to surround the upper portion of a PC soma and often its lower portion (Fig. 6B). Occasionally, a tendrill fiber surrounding a soma was also given off directly from the thick branch running on the soma. The number of swellings on these tendrill fibers around a target PC soma was 12.0 ± 3.4 ($n = 32$), which was about 4.8% of the total swellings of a CF.

Thin retrograde collaterals reentering the PC and granular layers from a CF terminal arborization

We observed thin retrograde collaterals (Scheibel and Scheibel, 1954) originating from a CF terminal arborization and reentering the PC and granular layers. These collaterals originated from somal portions (Fig. 6C, arrows; Fig. 7A) and dendritic portions in the deep molecular layer less than about 30 μm from the PC layer (Fig. 7B,C). These collaterals were rather short (<100 μm) and bore a terminal swelling and sometimes a few en passant swellings, and seldom had ramifications. In counterstained preparations, some swellings on retrograde collaterals in the PC layer apparently touched a PC which was not the target of the CF terminal arborization (Fig. 7C, arrow). Among 490 CFs that were labeled with small and large

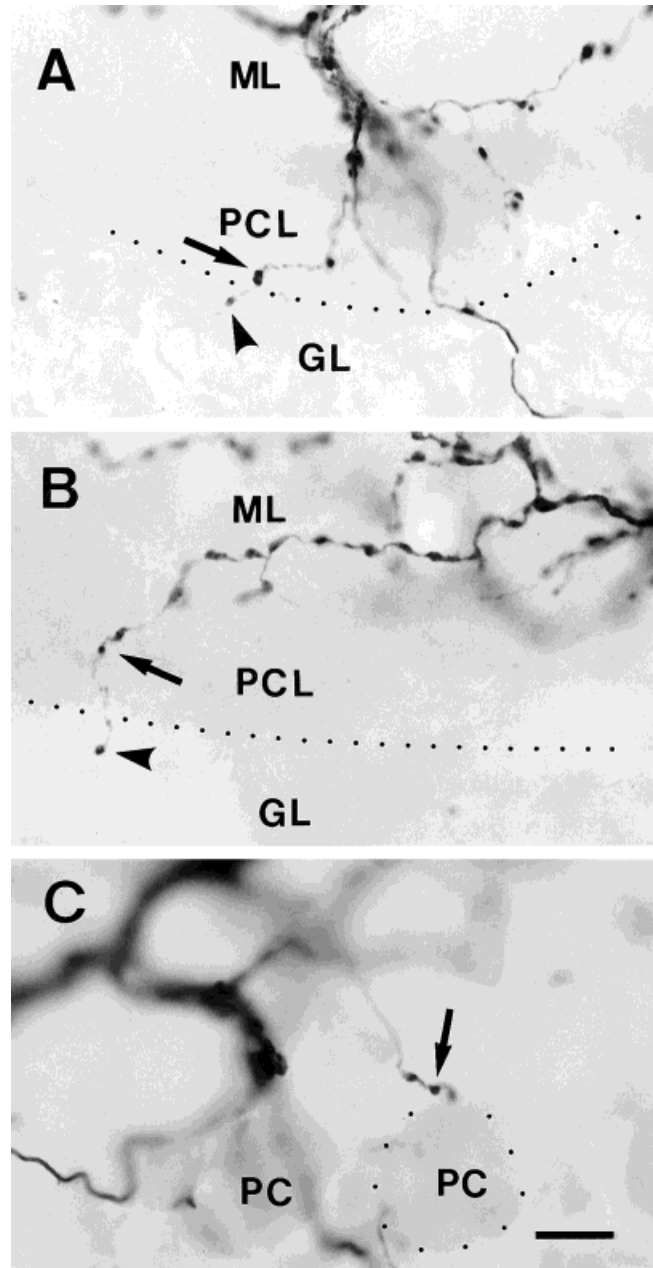


Fig. 7. Photomicrographs of thin retrograde collaterals reentering the Purkinje cell (PC) and granular layers from terminal arborization of a climbing fiber. **A:** Collateral given off from around a soma of a PC. **B:** Collateral given off from around the distal portion of a thick dendrite. Dotted lines in A and B indicate the border between the PC and granular layers. Arrows in A–C indicate swellings in the PC layer; arrowheads in A and B indicate swellings in the granular layer. **C:** Collateral given off from around a thick dendrite and swellings (arrow) in close apposition to a PC (dots). The section in C was weakly counterstained. The surface of the cerebellar cortex is to the top in each figure. GL, granular layer; ML, molecular layer; PCL, Purkinje cell layer. Scale bar = 10 μm in C (applies to A–C).

injections of tracer into the IO, 221 had retrograde collaterals originating from a somal portion of the CF terminal arborization, and 38 had retrograde collaterals originating from a dendritic portion of the CF terminal arborization.

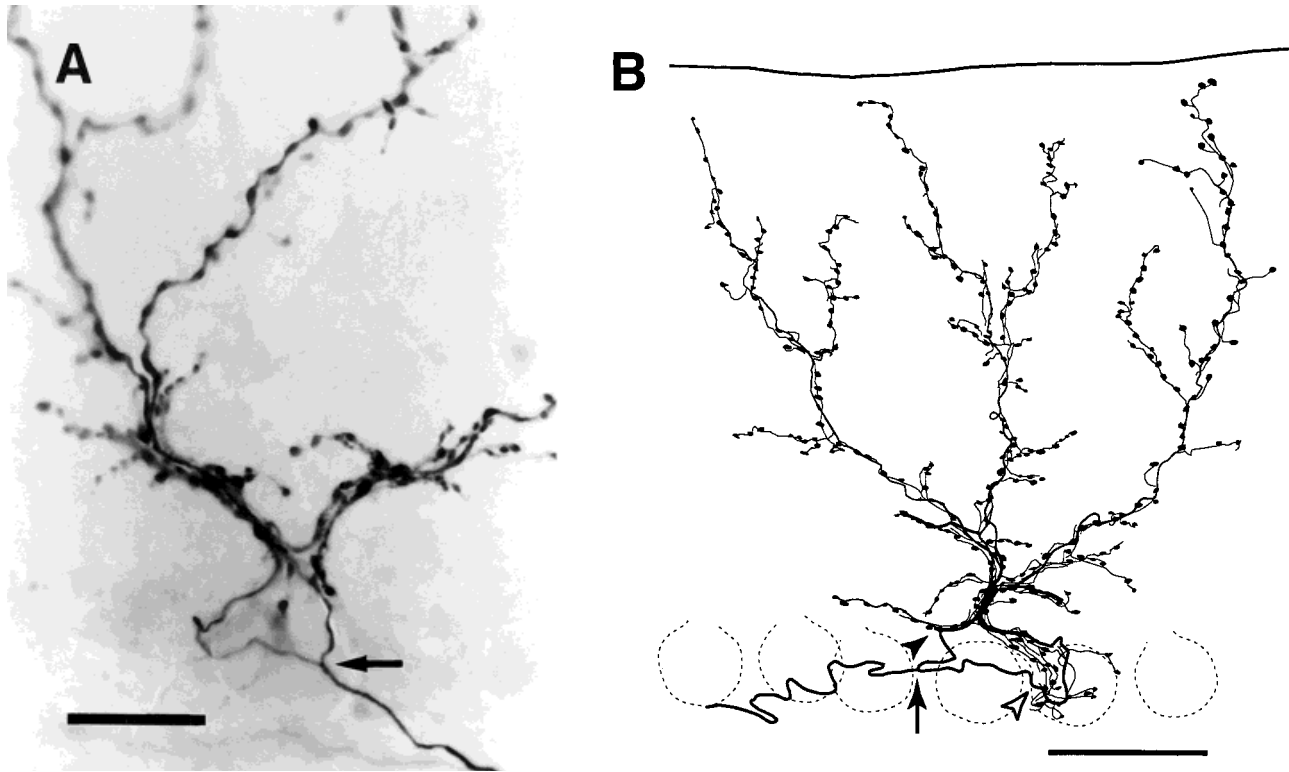


Fig. 8. Pseudo-double innervation of a Purkinje cell (PC) by thick branches of olivocerebellar (OC) axons. **A:** Photomicrograph of two thick branches of an OC axon (arrow) forming a combined single terminal arborization. **B:** Reconstruction of two thick branches of another OC axon (arrow) forming a single combined terminal arboriza-

tion. One of the branches reached a soma of a PC (open arrowhead), whereas the other reached a dendrite of the same PC (filled arrowhead) and ran to the proximal portion. Scale bars = 20 μm in A; 50 μm in B.

Possibility of double innervation of a single PC by CFs

To examine whether a terminal arborization on a single PC is always formed by a single thick branch of an OC axon, we observed 523 CFs in three experiments with a large volume of tracer and where more than 100 OC axons were labeled in each cerebellum. We found only two exceptional cases. In one case, a thick branch of an OC axon bifurcated in the PC layer into two daughter thick branches (Fig. 8A, arrow), which reached the proximal portion of the main dendrite of a single PC, and gave rise to tendrill fibers to form a single combined terminal arborization. In the other case, a thick branch of an OC axon bifurcated in the PC layer (Fig. 8B, arrow). One of the two daughter thick branches reached a PC at its soma after running for about 40 μm (Fig. 8B, open arrowhead). The other thick branch reached the same PC at its dendrite after running for about 20 μm (Fig. 8B, filled arrowhead), ran along the dendrite to the proximal main dendrite, and met with the other branch to form a single combined terminal arborization. In both cases, stalk fibers originating from the two thick branches ran in parallel along some portions of proximal dendrites; therefore, it was difficult to determine dendritic territories innervated by the two thick branches. However, the distal portions of the PC thick dendrites were innervated by either of the thick branches. Except for these two cases, a terminal arborization always originated from a single thick branch of an OC axon. However, the innervation shown in Figure 8 would be

functionally identical to the normal innervation of a PC by a single IO neuron, because the two thick branches originated from a common stem axon in each case. Therefore, they were designated as "pseudo-double innervation."

Branches of CF terminal arborizations within the molecular layer

The dense terminal arborization of a CF occupied a width of about 8 μm in transverse sections (Fig. 9A–C), which was compatible with the thickness of a PC dendritic tree (Ito, 1984), and was consistent with the morphology of a CF terminal arborization surrounding thick dendrites of a PC. A CF terminal arborization wider than this could be due to a slight tilt or curvature of the dendritic plane, but never indicated innervation of multiple PCs by a CF. Closer observation revealed that several very thin short branches (diameter, 0.2 μm or less; length, about 20 μm or less) running in the transverse plane were given off from some points of a terminal arborization (Fig. 9, arrowheads). These branches, called "transverse branchlets" here, have not been clearly described in previous studies. Swellings on transverse branchlets were often relatively small (diameter < 0.8 μm ; Fig. 9B). Although no transverse branchlets were visible in some CF terminal arborizations, this finding seemed to be attributable to incomplete labeling.

A few swellings of each CF terminal arborization were usually seen to touch somata of interneurons in the molecular layer in counterstained parasagittal and coro-

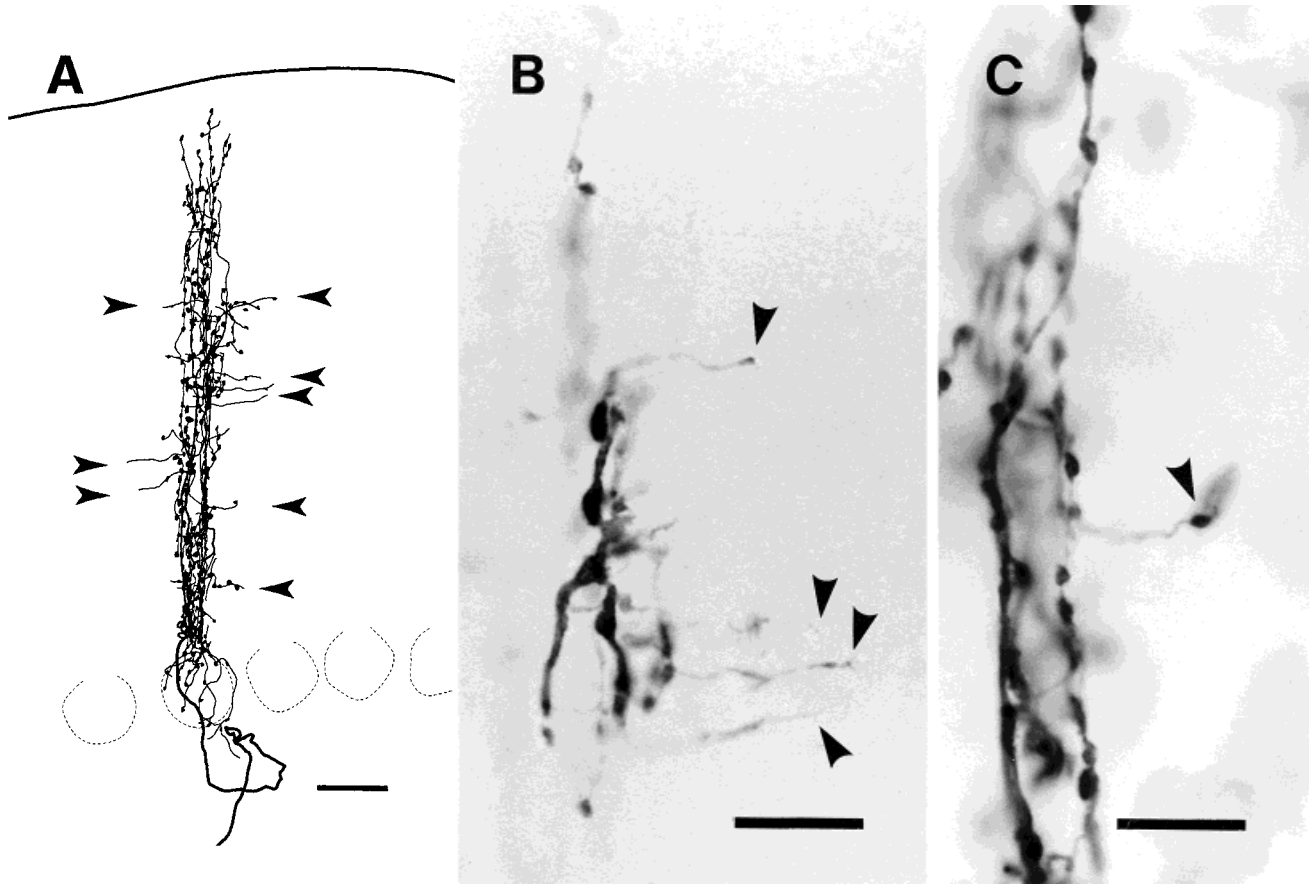


Fig. 9. Climbing fiber terminal arborizations in transverse sections. **A:** Reconstruction of a terminal arborization from four sections. Arrowheads indicate transverse branchlets. Because a dendritic tree of a PC was neither completely flat nor exactly perpendicular to the section, the reconstructed terminal arborization had a width much wider than that seen in a single section. **B:** Photomicrograph of

terminal arborizations and transverse branchlets (arrowheads). **C:** Photomicrograph of a transverse branchlet touching an interneuron with a swelling in a counterstained section. The surface of the cerebellar cortex is to the top in each panel. Scale bars = 20 μm in A; 10 μm in B,C.

nal sections (Fig. 10A). These swellings were borne on tendril fibers within the terminal arborization of a CF. Swellings on transverse branchlets were also seen to occasionally touch counterstained somata of interneurons in transverse sections (Fig. 9C). It was difficult to recognize transverse branchlets in sections that were not perpendicular to the PC dendritic plane.

Thin collaterals of OC axons

Thin collaterals, which were given off from stem axons and thick branches of OC axons before they formed CF terminal arborizations, were more abundant in terms of the number per OC axon than thick branches. For convenience of description, they were classified into three types according to their main termination sites: (1) white matter in the ICP, (2) the cerebellar nuclei, and (3) the cerebellar granular layer.

When labeled thin axons bearing swellings in the ICP ($n = 23$), cerebellar nuclei ($n = 42$), and the granular layer ($n = 81$) were traced proximally, they were always found to be collaterals of OC axons, which gave rise to some CFs. This finding indicated that all of the axon terminals in the ICP, the cerebellar nuclei, and the granular layer were derived from OC axons terminating as CFs in the cerebel-

lar cortex, and none of the OC axons specifically terminated in the ICP, the cerebellar nuclei or the granular layer without sending CFs to the cerebellar cortex.

Collaterals terminating in the white matter of the ICP

About half of the OC axons reconstructed throughout the ICP (16 of 28, which included 16 axons that were completely reconstructed) had a single or occasionally a few thin collaterals in the ICP (both the rostral and caudal portions) near the junction to the cerebellum (Figs. 5, 10B). These collaterals were often the first collaterals of OC axons. They bore a single terminal swelling and sometimes several *en passant* swellings. The average number of swellings per thin collateral and per OC axon in the ICP was 2.8 ± 2.5 ($n = 18$) and 1.8 ± 2.5 ($n = 28$), respectively. The diameters of these collaterals and the swellings were 0.2–0.3 μm and mostly 0.8–1.4 μm , respectively. Swellings on these collaterals were localized within the white matter of the ICP. In counterstained sections, most of the swellings did not touch somata or proximal dendrites of neurons. However, some of the swellings touched small and medium neurons scattered in the white matter of the ICP (Fig. 10B).

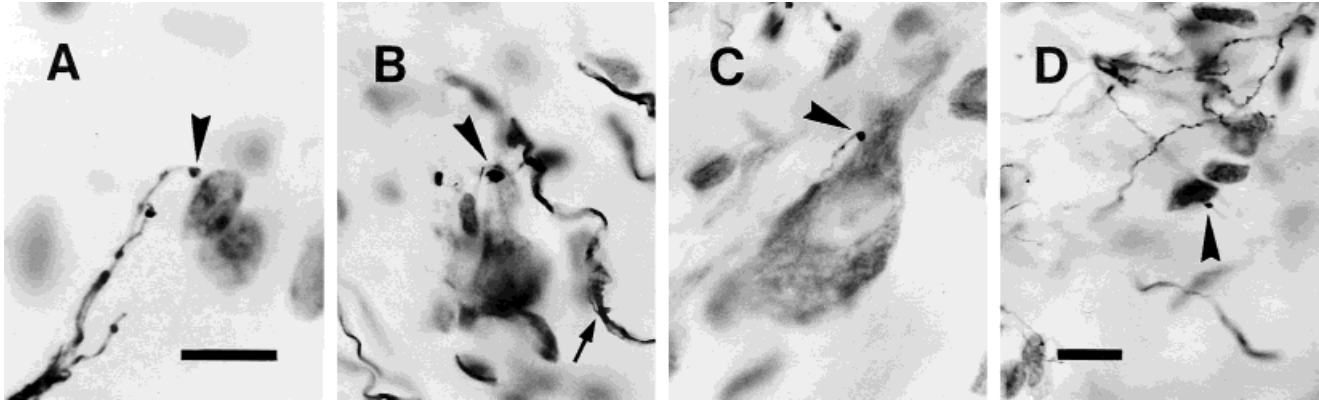


Fig. 10. Photomicrographs of swellings touching neurons in counterstained sections. **A:** Swelling on a terminal arborization of a climbing fiber that touched interneurons in the molecular layer in a sagittal section. **B:** Swelling touching the proximal portion of a dendrite of a medium neuron scattered in the white matter of the inferior cerebellar peduncle. This swelling was of a short thin collat-

eral given off from an olivocerebellar axon (arrow). **C:** Swelling touching a soma of a large neuron in the fastigial nucleus. **D:** Swelling touching a soma of a small neuron in the fastigial nucleus. Arrowheads in A–D indicate swellings touching stained neurons. Scale bars = 10 μm in A; 10 μm in D (applies to B–D).

Collaterals terminating in the cerebellar nuclei

Thin collaterals to the cerebellar nuclei were observed in 20 of 22 OC axons that were reconstructed throughout the deep cerebellar white matter. Each of these 20 axons had one ($n = 15$), two ($n = 3$, Fig. 11B), three ($n = 1$), or six ($n = 1$) collaterals (Fig. 11A) (1.4 ± 1.2 collaterals per OC axon). Each OC axon innervated only a single cerebellar nucleus.

Nuclear collaterals were given off from stem OC axons or their thick branches in the deep white matter near or within the cerebellar nuclei (Fig. 11A,B). Because thin collaterals terminating in the granular layer were also sometimes given off at this portion of OC axons, collaterals could not be identified as terminating in the cerebellar nuclei without tracing them to their terminals. The diameters of nuclear collaterals were 0.2–0.3 μm . Ramification of collaterals in the termination area in the cerebellar nucleus was more frequent than that of other thin collaterals in the granular layer and the ICP. Terminal branches bore several *en passant* swellings and terminal swellings. The diameters of the swellings were mostly 0.8–1.4 μm . The average number of swellings per OC axon was 54.0 ± 66.0 ($n = 22$).

In counterstained sections, some swellings touched somata and proximal dendrites of both large (Fig. 10C) and small neurons (Fig. 10D). However, many of the swellings did not touch the stained portion of the neurons, indicating that they presumably touched more distal dendrites. We observed that some OC axons gave rise to thin collaterals terminating in the vestibular nucleus, which were similar to cerebellar nucleus collaterals morphologically.

Collaterals terminating mainly in the granular layer

Thin collaterals were frequently given off from stem or thick branches of OC axons in the deep white matter and in the folial white matter (Figs. 5D, open arrowheads; 12A,B). These thin collaterals sometimes ran parallel to their parent axon at the beginning, but eventually separated from it (Fig. 12B). They occasionally bifurcated in the white matter into thin daughter collaterals, the diam-

eters of which were similar to those of their parent thin collaterals. Some of these thin collaterals terminated in the white matter with a solitary terminal swelling (Fig. 12A, filled circles; Fig. 13A) or a few *en passant* swellings and a terminal swelling (diameter of swellings, 0.8–2 μm). The rest of these thin collaterals entered the granular layer. Thin collaterals were also given off from thick branches in the granular layer (Fig. 12C, arrowheads) and infrequently even in the PC layer before the thick branches reached a target PC (Fig. 6D, arrow). Thin collaterals arising in the white matter and different layers of the cerebellar cortex had similar morphologic characteristics in the granular layer.

These thin collaterals took winding courses for a distance of usually less than several hundred micrometers in the granular layer with a few or no ramifications. They bore a terminal swelling, *en passant* swellings (Fig. 13B), and occasionally a swelling on a short branchlet in the granular layer (number of swellings per collateral, 1–21). Swellings were sparsely distributed, and no dense terminal arborizations were formed. The diameters of the swellings were 0.5–2 μm , mostly 0.8–1.4 μm .

Swellings were most dense in the upper portion of the granular layer, but were seen at all depths in that layer. In counterstained preparations, some swellings in the granular layer seemed to make a contact with a soma of a presumed Golgi cell (Fig. 13C), which was identified by its purple-colored soma that was much larger than a granule cell soma and smaller than a PC soma. Other swellings were located among a dense aggregation of blue-colored granule cells. Thin collaterals in the granular layer sometimes extended as far as the PC layer and bore some swellings there (Fig. 12B,D, arrows). Some of these swellings apparently touched PCs (Fig. 13D), which were not the targets of CFs from the same OC axon. However, these thin collaterals extending into the PC layer never joined (cf. Fox et al., 1969) or produced a CF terminal arborization in the molecular layer.

Thin collaterals usually terminated in the same lobe and in the same thin parasagittal zone as CFs originating from the same OC axons (Fig. 5D). In the longitudinal

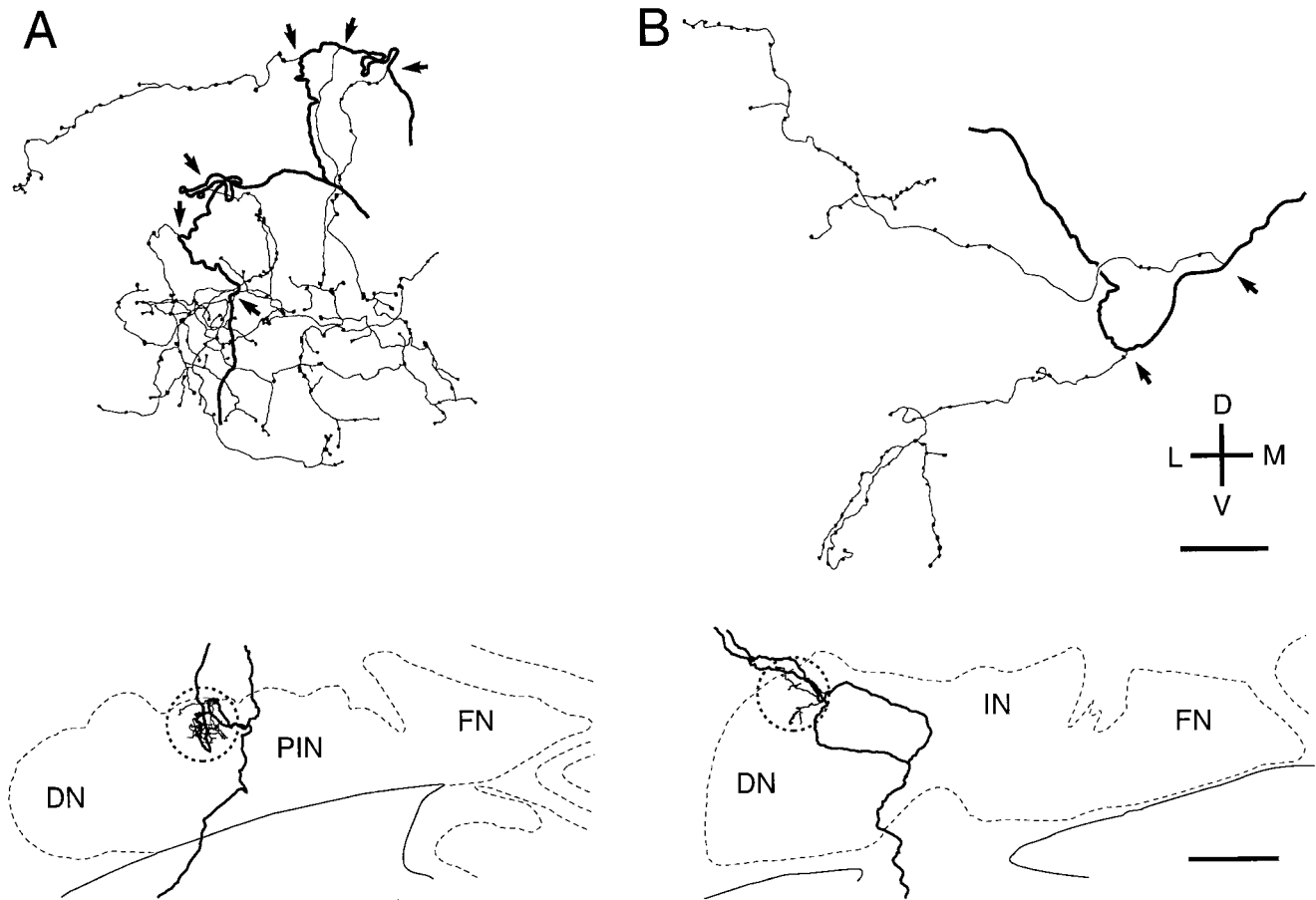


Fig. 11. Reconstructed collaterals of single olivocerebellar (OC) axons terminating in the cerebellar nuclei illustrated at medium (top) and low (bottom) magnifications. **A:** Nuclear collaterals originating from a single OC axon projecting to zone C2 in the left cerebellum, reconstructed in the coronal plane from 40 serial sections. **B:** Nuclear collaterals of another OC axon projecting to zone D1 in the left hemisphere, reconstructed in the coronal plane from 28 serial sections.

Arrows indicate branching points. Dotted circles in the bottom drawings indicate the termination areas in the cerebellar nuclei. IN, interposed cerebellar nucleus; DN, dentate nucleus; FN, fastigial nucleus; PIN, posterior interposed cerebellar nucleus; D, dorsal; V, ventral; L, lateral; M, medial. Scale bars = 50 μ m for top drawings, 0.5 mm for bottom drawings.

direction, however, terminals of thin collaterals were not necessarily adjacent to these CFs, but were sometimes apart from them by more than 1 mm (Fig. 12A).

The number of granular layer thin collaterals ranged from 3 to 16 (average, 8.5 ± 3.7 , $n = 8$ axons completely reconstructed, including thin collaterals) per OC axon. The number of branchings of thin collaterals from stem OC axons or their thick branches in the deep white matter, proximal folial white matter, distal folial white matter, and granular layer was 26 (38%), 15 (22%), 13 (19%), and 14 (21%), respectively, in a total of 68 branchings in eight OC axons that were reconstructed completely. The average number of swellings on thin collaterals in the white matter, granular layer, and PC layer per OC axon was 3.5 ± 2.1 , 28.0 ± 8.0 , and 0.9 ± 1.1 ($n = 8$ axons), respectively.

To estimate further the relative number of swellings in the granular layer, the number of swellings was simply counted in lobules VI and VII, in which labeled CFs were seen, in 24 counterstained parasagittal sections in two animals with large volumes of the tracer injected into the IO. The total number of labeled CFs was 387, which corresponded to 63.4 OC axons, assuming that a single OC axon makes 6.1 CFs on average. The number of swellings

in the granular layer was 1,639, which was equivalent to $1,639/63.4 = 25.8$ swellings per OC axon. This approximately equaled the average number of swellings counted in single axons in the granular layer (28.0). The number of swellings belonging to thin collaterals in the PC layer, but not to terminal arborizations of CFs, was 215, which was equivalent to $215/63.4 = 3.4$, swellings per OC axon. This was slightly larger than the value in the above paragraph (0.9), which was presumably because swellings belonging to thin retrograde collaterals (see earlier section) was included in this value.

DISCUSSION

As unitary functional entities, single neurons and axons have been important subjects of morphologic and physiological studies on the nervous system. However, previous morphologic studies on single CFs and OC axons have only clarified localized features of their morphology in the cerebellar cortex (Ramón y Cajal, 1911; Scheibel and Scheibel, 1954; Fox et al., 1969), the cerebellar nuclei (Van der Want et al., 1989; Sugihara et al., 1996), and the IO (Ruigrok et al., 1990). Although anterograde (Groenewe-

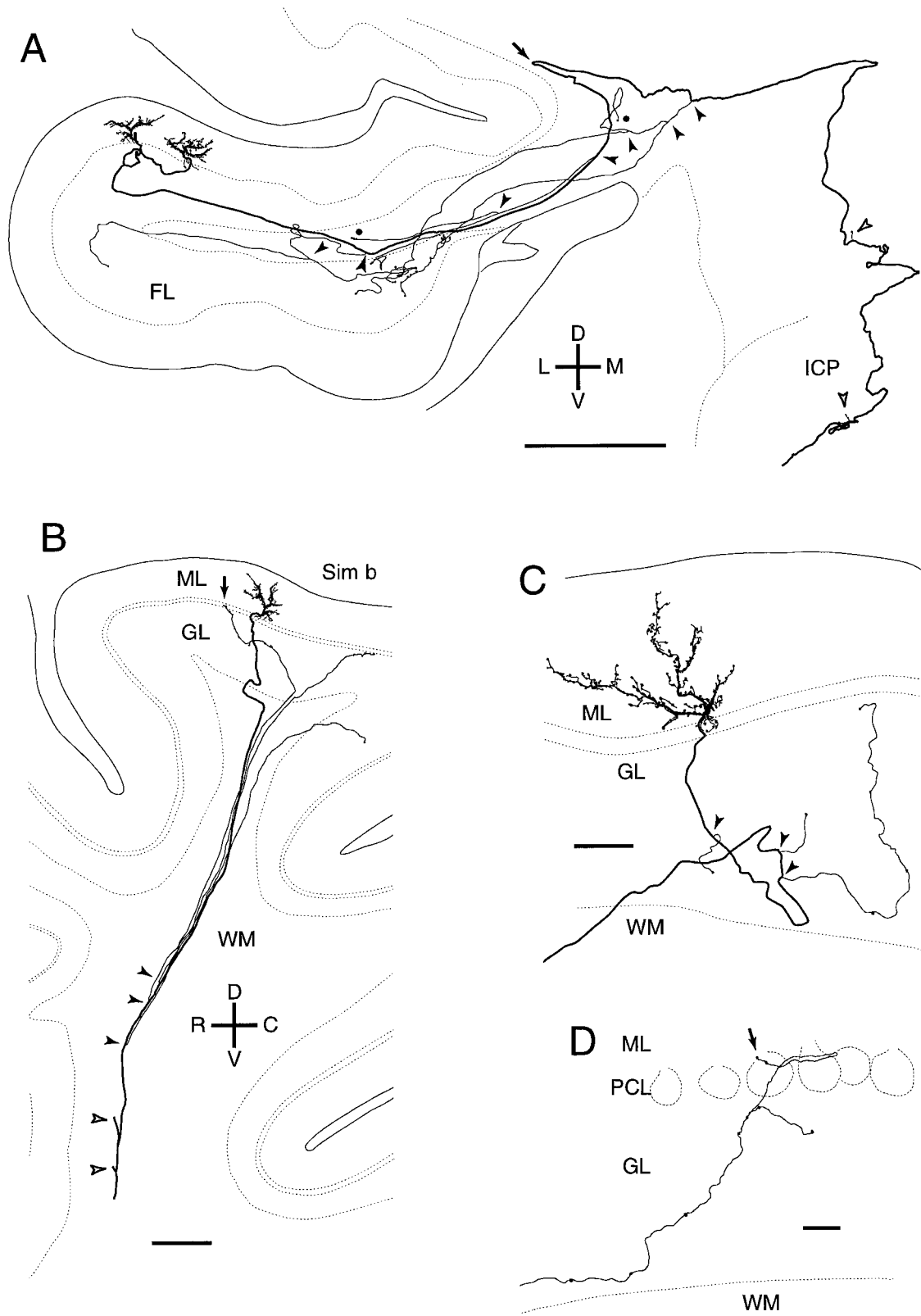


Fig. 12. Reconstructed thin collaterals terminating mainly in the granular layer. **A:** Trajectory of an olivocerebellar (OC) axon that terminated in the flocculus reconstructed in the coronal plane from 65 sections. This axon had two climbing fibers, two thin collaterals terminating in the inferior cerebellar peduncle (ICP) (open arrowheads), two thin collaterals terminating in the cerebellar white matter (filled circles), and several thin collaterals terminating in the granular layer. Filled arrowheads indicate branching points. An arrow indicates hairpin-shaped returning. **B:** Three thin collaterals given off from a thick branch of an OC axon in the folial white matter (filled arrowheads). Reconstructed in the parasagittal plane from 10 coronal sections. An arrow indicates swellings in the Purkinje cell (PC) layer.

Two thick branches of this axon were not drawn for clarity (open arrowheads). **C:** Collaterals given off from a thick branch of an OC axon in the granular layer (filled arrowheads). Reconstructed from five coronal sections. **D:** Thin collateral of an OC axon that bore swellings not only in the granular layer but also in the PC layer. Reconstructed from two parasagittal sections. An arrow indicates swellings in the PC layer. FL, flocculus; ICP, inferior cerebellar peduncle; ML, molecular layer; PCL, Purkinje cell layer; Sim b, sublobule b of the simple lobule; GL, granular layer; WM, white matter; D, dorsal; V, ventral; R, rostral; C, caudal; L, lateral; M, medial. Scale bars = 500 μ m in A; 200 μ m in B; 50 μ m in C; 20 μ m in D.

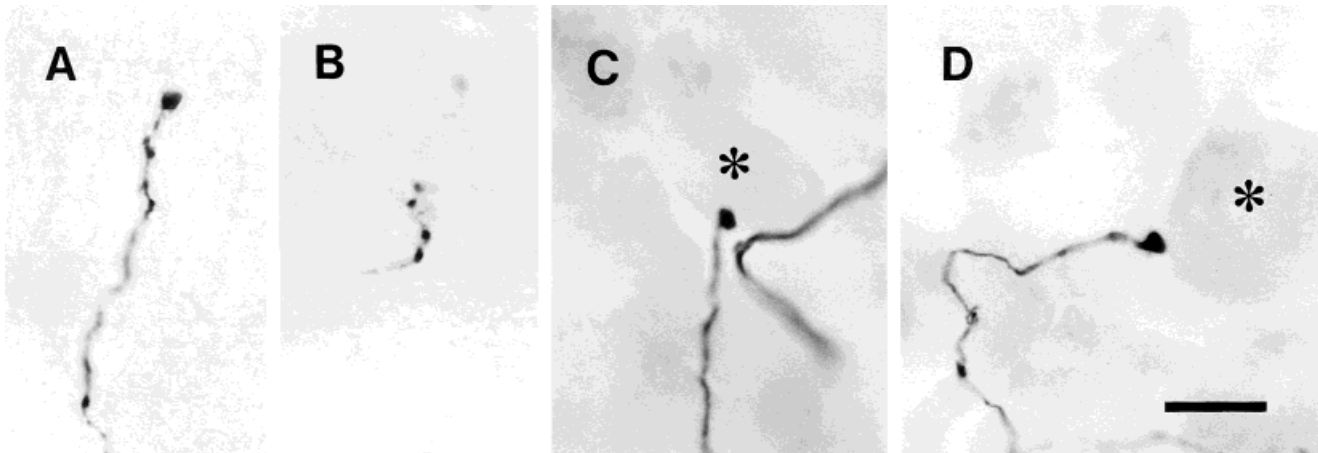


Fig. 13. Photomicrographs of swellings of thin collaterals of olivocerebellar axons in the cerebellar white matter and cortex. **A:** Terminal swelling in the white matter. **B:** *En passant* and terminal swellings in the granular layer. **C:** Terminal swelling touching a soma of a

presumed Golgi cell. **D:** Terminal swelling touching a soma of a Purkinje cell. The surface of the cerebellar cortex is to the top in each panel. Asterisk in C, presumed Golgi cell. Asterisk in D, Purkinje cell. Scale bar = 10 μ m in D (applies to A–D).

gen and Voogd, 1977; Van der Want et al., 1989; Sugihara et al., 1993) and retrograde (Brodal et al., 1980; Rosina and Provini, 1983; Azizi and Woodward, 1987; Hrycyshyn et al., 1989) labeling studies of OC axons have shown the general pathway of OC axons and the topographical pattern of OC projection, they could not reveal the morphology of single OC axons, because they labeled a large number of neurons as a whole. On the other hand, electrophysiological studies have demonstrated axonal branchings and receptive field organization in the OC projection by investigating the projection of single OC axons or a group of functionally related OC axons (Faber and Murphy, 1969; Armstrong et al., 1973; Ekerot and Larson, 1982). However, these studies could not necessarily provide quantitative data on OC axons, because they could detect neither all CFs nor any thin collaterals of an OC axon. In these respects, the entire detailed morphology of single OC axons described in the present study should contribute significantly to future physiological studies on the OC system as basic anatomic background. The spatial distribution pattern of CFs of a single OC axon varied in the cerebellar cortex (see Figs. 4A,B, 5D, 12A), and its elucidation would require further studies. The present results suggest that the morphology of single axons provides an important clue for understanding the organization of the compartmentalization of the cerebellar cortex by OC projection.

Axonal pathways and laterality of OC projection

The pathways of individual OC axons in the brainstem revealed in the present study are largely consistent with the results of previous experiments with mass labeling (Voogd and Bigaré, 1980; Wiklund et al., 1984). The arrangement of the rostral and caudal paths of OC projection within the ICP at the junction to the cerebellum detailed in the present study seems basically similar to the arrangement in the cat (Voogd and Bigaré, 1980).

Concerning the entrance to the cerebellum, the present study showed that a very small number of neurons in the medial DMCC presumably send their axons through the ipsilateral ICP, whereas virtually all other axons run

through the contralateral ICP. Fusion of the left and right IO occurs only at the DMCC in the rat (de Zeeuw et al., 1996). Therefore, as a possible interpretation, these ipsilateral projections might occur due to the accidental migration of DMCC neurons to the opposite side.

We also found ipsilateral cerebellar projection of IO neurons formed by double-crossing axons. These axons would probably explain the presence of ipsilateral projection suggested previously by anterograde (Chan-Palay et al., 1977) and retrograde (Brown, 1980; Hrycyshyn et al., 1989) labeling studies and an electrophysiological study (Yamamoto et al., 1986). It seems that neurons with bilateral projection, although small in number, are generally present in several subnuclei of the IO, since Brown (1980) and Hrycyshyn (1989) found some in the rostral principal olive and rostral dorsal accessory olive, and we found some in the medial accessory olive. Double-crossing projection of OC axons has been found after cutting the ICP in the newborn period (Angaut et al., 1985; Sherrard et al., 1986). Ipsilateral innervation by some OC axons is transiently formed in young animals, although the pathway is not clear (López-Román et al., 1993). Therefore, double-crossing projection in the adult cerebellum might be reminiscent of the projection in the newborn.

Ramification of OC axons

The average number of CFs per OC axon in this study (6.1) was close to the number (n = about 7) inferred in the rat by counting the total number of IO neurons and PCs (Schild, 1970). Previous studies could not determine where branchings of CFs mainly occurred (Ramón y Cajal, 1911; Fox et al., 1969; Desclin, 1974; Rossi et al., 1991; Sugihara et al., 1996). In the present study, most of the CFs and thin collaterals arose in the folial and deep white matter. Even CFs that terminated adjacent to each other occasionally arose in the deep white matter and the proximal folial white matter (Figs. 4A, 5D). This origin may be related to the development of the cerebellum. Maturation and foliation of the cerebellar cortex occur mainly in postnatal periods after the innervation of PCs by CFs has been

established (Altman and Bayer, 1997). Therefore, although the folium extends toward the apex, the branching points might be left behind in the deep and proximal white matter.

Comparative morphology of CFs and thin collaterals of OC axons

This study revealed that OC axons gave rise to a number of thin collaterals, which have not yet been described, except for nuclear collaterals (Wiklund et al., 1984; Van der Want and Voogd, 1987; Van der Want et al., 1989; Sugihara et al., 1996) and collaterals in the cerebellar cortex (Fox et al., 1969; Chan-Palay and Palay, 1971; Palay and Chan-Palay, 1974; Rossi et al., 1991). Because of the abundance of these non-CF thin collaterals, it seems better to make a distinction between the terms CFs and OC axons, as was done in the present study. The general morphology of terminations of these thin collaterals in the ICP, the cerebellar nuclei and the granular layer and retrograde collaterals in the cerebellar cortex was quite similar. They did not make dense terminal arborization, because branching was infrequent and swellings were sparse. In comparison, CF terminal arborizations had a very dense distribution of swellings. However, individual swellings in the molecular layer were not significantly different from those in the cerebellar nuclei and other areas. Both swellings were globose or polygonal in shape. The sizes of swellings on CF terminal arborizations largely overlapped those for swellings on thin collaterals in the ICP, cerebellar nuclei and granular layer. The tendril fibers of CF terminal arborizations were similar in diameter to thin collaterals. We did not observe large effluence-type terminals about 12–15 μm long or CF glomerulus in the granular layer of the adult rat cerebellum (Chan-Palay and Palay, 1971).

Projection of OC axons in the molecular and PC layers

The present findings on the innervation of PC dendrites by CFs are basically similar to those in previous reports (Ramón y Cajal, 1911; Fox et al., 1969; Palay and Chan-Palay, 1974; Rossi et al., 1991; Llinás and Walton, 1998). The number of swellings on a single CF in the present study ($n = 250$) is comparable to a previously measured value in the rat ($n = 288$; Rossi et al., 1993) and larger than a value in the frog ($n =$ about 100 beads; Llinás et al., 1969).

Contact of interneurons by some swellings of CFs in the molecular layer was emphasized by Scheibel and Scheibel (1954) in their study with Golgi staining. The present study confirmed such contact at the light-microscopic level and also showed close opposition with interneurons of some swellings of transverse branchlets. This study made the first clear description of transverse branchlets. The occasional transverse short elongation of fine fibers reported previously (Rossi et al., 1991) may be what we call transverse branchlets. Despite the contact of CF terminals on interneurons, the formation of a synaptic structure between them has been excluded in an electron-microscopic study (Hámori and Szentágothai, 1980). On the other hand, electrophysiological studies have demonstrated a weak excitatory effect of CFs on some interneurons (Eccles et al., 1966b; O'Donoghue et al., 1989). Thus, the nature of the transmission from CFs to molecular layer interneurons remains unclear.

Besides the innervation of proximal dendrites of PCs, the innervation of a PC soma by CFs in adult animals was originally described to be very weak and restricted to the upper portion of the soma, or absent (Ramón y Cajal, 1911). Later studies did not describe any details of the somal innervation by CF terminal arborizations (Scheibel and Scheibel, 1954; Fox et al., 1969; Palay and Chan-Palay, 1974; Rossi et al., 1991). An electron-microscopic study showed that varicosities of a tendril fiber of a CF form synaptic contact with thorns from a PC soma, but these synapses were reportedly rare (Chan-Palay and Palay, 1971). However, the present study showed that a CF terminal arborization always surrounds a PC soma and bears about 5% of the total swellings of the CF. This difference may be partly due to technical improvements in labeling, because swellings around a PC soma were borne on thin and relatively long tendril fibers. Our findings suggest that, like PC thick dendrites, the PC soma is also a primary target of a CF.

Despite the description by Scheibel and Scheibel (1954) of types of retrograde collaterals, earlier and later studies described only one type of a retrograde collateral that extended down to the granular layer from the PC somal portion of a CF terminal arborization (Ramón y Cajal, 1911; Fox et al., 1969; Palay and Chan-Palay, 1974; Rossi et al., 1991). We confirmed the existence of retrograde collaterals that originated from the PC dendritic portion of a CF terminal arborization and contact of swellings of retrograde collaterals with a different PC soma under light microscopy, which were first described by Scheibel and Scheibel (1954).

Projection of OC axons in the granular layer

Terminals in the granular layer were originated either from thin collaterals of OC axons or from retrograde collaterals of CF terminal arborizations. The former was the main source of swellings in the granular layer. The morphology of the thin collaterals in the present study was consistent with "globose varicosities connected by a fine thread" as described in Golgi preparations and electron micrograms (Chan-Palay and Palay, 1971). Swellings of thin collaterals (about 1.7% of the total number of swellings per OC axon) were most abundant in the upper portion of the granular layer just underneath the PC layer, in which Golgi cells are usually located. Furthermore, some of these swellings were observed to touch presumed Golgi cells in the present study. Thus, the present results were consistent with electron-microscopic findings on the innervation of somata of Golgi cells by thin collaterals (Hámori and Szentágothai, 1966; Chan-Palay and Palay, 1971; Llinás and Walton, 1998). The target of swellings in the lower granular layer may also be Golgi cells, because Golgi cells are found at all depths in the granular layer (Ramón y Cajal, 1911). Some swellings in the granular layer were not apparently touching a Golgi cell soma in our preparation. The targets of these swellings were unknown, but Golgi cell dendrites may be one possibility. Possible targets of swellings in the white matter may also be Golgi cell dendrites, because they sometimes extend down to the white matter (Ramón y Cajal, 1911). Inferior olive stimulation has been shown electrophysiologically to have a weak direct excitatory effect on Golgi cells (Eccles et al., 1966b), which may correspond to the present findings. However, another study showed no excitatory effect, but rather a slow inhibitory effect, possibly mediated through PCs and

other interneurons (Schulman and Bloom, 1981). Thus, CF input to Golgi cells still needs to be re-examined electrophysiologically.

Projection of OC axons in the cerebellar nuclei and the ICP

Ninety-one percent of the OC axons examined had nuclear collaterals. Because the possibility of insufficient staining could not be excluded, this percentage may be an underestimation. The ratio of swellings in the cerebellar nuclei versus those of CF terminal arborizations was about 0.036 in individual OC axons in the present study. However, because the volume of the cerebellar nuclei is much smaller than that of the cerebellar cortex, and because significant convergence of input from OC axons to cerebellar nucleus neurons is present (Sugihara et al., 1996), cerebellar nucleus projection of OC fibers can still be functionally important. Some swellings seemed to make contact with the soma and the proximal portions of dendrites of large neurons in the present study, which was consistent with the steep rising phase of postsynaptic excitatory potentials in cerebellar nucleus neurons after IO stimulation (Kitai et al., 1977; Shinoda et al., 1987). Although intracellular potentials were presumably recorded only from large output neurons in the cerebellar nuclei, the present study suggested that small neurons were also innervated by OC axons. Because many swellings were presumably in contact with non-thionine-labeled distal portions of neurons, as shown in an electron microscopic study (Van der Want and Voogd, 1987), the relative extent of the innervation of large and small neurons was not clear in the present study. Collateral innervation of neurons scattered in the white matter of the ICP was found for the first time in the present study. However, the nature of these neurons remains unknown.

One-to-one relationship and possible exceptions in OC projection

Virtually all possible types of double innervation except for "pseudo-double innervation" were excluded in the present study, and pseudo-double innervation should still be functionally identical to one-to-one innervation. Therefore, a one-to-one relationship between a CF and a PC seems to be a fundamental characteristic of OC projection in the adult cerebellum. However, the present study suggests the possibility that swellings of thin collaterals of an OC axon might make contact with a PC that is not the target of CFs originating from the same OC axon. First, swellings of retrograde collaterals made contact with a different PC (Fig. 7C). Second, thin collaterals in the granular layer occasionally extended to the PC layer and bore swellings there, some of which apparently touched a PC (Fig. 13D). The PCs that might be innervated by these types of thin collaterals surely receive dense innervation by a CF originating from a different OC axon. Therefore, these types of contact, if shown to form synapses, should constitute multiple innervation. Thus, the projection of OC axons to PCs could be considered to consist of (1) strong one-to-one primary innervation by CFs and (2) possible multiple subsidiary innervation by thin collaterals. The existence and function of the latter type of synaptic contact will have to be examined further both electrophysiologically and electron microscopically.

ACKNOWLEDGMENTS

Y.S. was supported by CREST (Core Research for Evolutional Science and Technology) of the Japan Science and Technology Corporation, and I.S. was a recipient of a Grants-in-Aid for Scientific Research from the Ministry of Education, Science and Culture of Japan.

LITERATURE CITED

- Altman J, Bayer SA. 1997. Development of the cerebellar system in relation to its evolution, structure, and functions. Boca Raton: CRC Press.
- Angaut P, Alvarado-Mallart RM, Sotelo C. 1985. Compensatory climbing fiber innervation after unilateral pedunculotomy in the newborn rat: origin and topographic organization. *J Comp Neurol* 236:161-178.
- Armstrong DM, Harvey RJ, Schild RF. 1973. The spatial organization of climbing fibre branching in the cat cerebellum. *Exp Brain Res* 18:40-58.
- Azizi SA, Woodward DJ. 1987. Inferior olivary nuclear complex of the rat: morphology and comments on the principles of organization within the olivocerebellar system. *J Comp Neurol* 263:467-484.
- Brodal A, Walberg F, Berkley KJ, Pelt A. 1980. Anatomical demonstration of branching olivocerebellar fibres by means of a double retrograde labelling technique. *Neuroscience* 5:2193-2202.
- Brown PA. 1980. The inferior olivary connections to the cerebellum in the rat studied by retrograde axonal transport of horseradish peroxidase. *Brain Res Bull* 5:267-275.
- Buisseret-Delmas C, Angaut P. 1993. The cerebellar olivo-corticonuclear connections in the rat. *Prog Neurobiol* 40:63-87.
- Chan-Palay V, Palay SL. 1971. Tendril and glomerular collaterals of climbing fibers in the granular layer of the rat's cerebellar cortex. *Z Anat Entwicklungsgesch* 133:247-273.
- Chan-Palay V, Palay SL, Brown JT, Van Itallie C. 1977. Sagittal organization of olivocerebellar and reticulocerebellar projections: autoradiographic studies with ³⁵S-methionine. *Exp Brain Res* 30:561-576.
- Crepel F, Mariani J, Delhaye-Bouchaud N. 1976. Evidence for a multiple innervation of Purkinje cells by climbing fibers in the immature rat cerebellum. *J Neurobiol* 7:567-578.
- Desclin JC. 1974. Histological evidence supporting the inferior olive as the major source of cerebellar climbing fibers in the rat. *Brain Res* 77:365-384.
- de Zeeuw CI, Lang EJ, Sugihara I, Ruijgrok TJH, Eisenman LM, Mugnaini E, Llinás R. 1996. Morphological correlates of bilateral synchrony in the rat cerebellar cortex. *J Neurosci* 16:3412-3426.
- Eccles JC, Llinás R, Sasaki K. 1966a. The excitatory synaptic action of climbing fibres on the Purkinje cells of the cerebellum. *J Physiol [Lond]* 182:268-296.
- Eccles JC, Llinás R, Sasaki K. 1966b. The inhibitory interneurons within the cerebellar cortex. *Exp Brain Res* 1:1-16.
- Ekerot C-F, Larson B. 1982. Branching of olivary axons to innervate pairs of sagittal zones in the cerebellar anterior lobe of the cat. *Exp Brain Res* 48:185-198.
- Faber DS, Murphy JT. 1969. Axonal branching in the climbing fiber pathway to the cerebellum. *Brain Res* 15:262-267.
- Fox CA, Andrade A, Schwyn RC. 1969. Climbing fiber branching in the granular layer. In: Llinás R, editor. *Neurobiology of cerebellar evolution and development*. Chicago: American Medical Association. p 603-611.
- Futami T, Shinoda Y, Yokota J. 1979. Spinal axon collaterals of corticospinal neurons identified by intracellular injection of horseradish peroxidase. *Brain Res* 164:279-284.
- Groenewegen HJ, Voogd J. 1977. The parasagittal zonation within the olivocerebellar projection. I. Climbing fiber distribution in the vermis of cat cerebellum. *J Comp Neurol* 174:417-488.
- Hámori J, Szentágothai J. 1966. Identification under the electron microscope of climbing fibers and their synaptic contacts. *Exp Brain Res* 1:65-81.
- Hámori J, Szentágothai J. 1980. Lack of evidence of synaptic contacts by climbing fibre collaterals to basket and stellate cells in developing rat cerebellar cortex. *Brain Res* 186:454-457.
- Hryciyshyn AW, Ghazi H, Flumerfelt BA. 1989. Axonal branching of the olivocerebellar projection in the rat: a double-labeling study. *J Comp Neurol* 284:48-59.
- Ito M. 1984. *The cerebellum and neural control*. New York: Raven Press.
- Itoh K, Konishi A, Nomura S, Mizuno N, Nakamura Y, Sugimoto T. 1979.

- Application of coupled oxidation reaction to electron microscopic demonstration of horseradish peroxidase: cobalt-glucose oxidase method. *Brain Res* 175:341–346.
- Kakei S, Shinoda Y. 1990. Parietal projection of thalamocortical fibers from the ventroanterior-ventrolateral complex of the cat thalamus. *Neurosci Lett* 117:280–284.
- Kitai ST, McCreary RA, Preston RJ, Bishop GA. 1977. Electrophysiological and horseradish peroxidase studies of precerebellar afferents to the nucleus interpositus anterior. I. Climbing fiber system. *Brain Res* 122:197–214.
- Krieger C, Shinoda Y, Smith AM. 1985. Labelling of cerebellar mossy fiber afferents with intra-axonal horseradish peroxidase. *Exp Brain Res* 59:414–417.
- Lang EJ, Sugihara I, Llinás R. 1996. GABAergic modulation of complex spike activity by the cerebellar nucleolivary pathway in rat. *J Neurophysiol* 76:255–275.
- Larsell O. 1952. The morphogenesis and adult pattern of the lobules and fissures of the cerebellum of the white rat. *J Comp Neurol* 97:281–356.
- Llinás RR, Walton KD. 1998. Cerebellum. In: Shepherd GM, editor. *The synaptic organization of the brain*, 4th ed. New York: Oxford University Press. p 255–288.
- Llinás R, Bloedel JR, Hillman DE. 1969. Functional characterization of neuronal circuitry of frog cerebellar cortex. *J Neurophysiol* 32:847–870.
- López-Román A, Ambrosiani J, Armengol JA. 1993. Transient ipsilateral innervation of the cerebellum by developing olivocerebellar neurons. A retrograde double-labelling study with fast blue and diaminidino yellow. *Neuroscience* 56:485–497.
- Mariani J. 1983. Elimination of synapses during the development of the central nervous system. *Prog Brain Res* 58:383–392.
- O'Donoghue DL, King JS, Bishop GA. 1989. Physiological and anatomical studies of the interactions between Purkinje cells and basket cells in the cat's cerebellar cortex: evidence for a unitary relationship. *J Neurosci* 9:2141–2150.
- Oscarsson O, Sjölund B. 1977. The ventral spino-olivocerebellar system in the cat. I. Identification of five paths and their termination in the cerebellar anterior lobe. *Exp Brain Res* 28:469–486.
- Palay SL, Chan-Palay V. 1974. Cerebellar cortex. Cytology and organization. New York: Springer-Verlag.
- Ramón y Cajal S. 1911. *Histologie du système nerveux de l'homme et des vertébrés*, vol II. Paris: Maloine.
- Rosina A, Provini L. 1983. Somatotopy of climbing fiber branching to the cerebellar cortex in cat. *Brain Res* 289:45–63.
- Rossi F, Wiklund L, Van der Want JJJ, Strata P. 1991. Reinnervation of cerebellar Purkinje cells by climbing fibers surviving a subtotal lesion of the inferior olive in the adult rat. I. Development of new collateral branches and terminal plexuses. *J Comp Neurol* 308:513–535.
- Rossi F, Borsello T, Vaudano E, Strata P. 1993. Regressive modifications of climbing fibres following Purkinje cell degeneration in the cerebellar cortex of the adult rat. *Neuroscience* 53:759–778.
- Ruigrok TJH, de Zeeuw CI, Van der Burg J, Voogd J. 1990. Intracellular labeling of neurons in the medial accessory olive of the cat: I. Physiology and light microscopy. *J Comp Neurol* 300:462–477.
- Scheibel ME, Scheibel AB. 1954. Observations on the intracortical relations of the climbing fibers of the cerebellum. A Golgi study. *J Comp Neurol* 101:733–763.
- Schild RF. 1970. On the inferior olive of the albino rat. *J Comp Neurol* 140:255–260.
- Schulman JA, Bloom FE. 1981. Golgi cells of the cerebellum are inhibited by inferior olive activity. *Brain Res* 210:350–355.
- Sherrard RM, Bower AJ, Payne JN. 1986. Innervation of the adult rat cerebellar hemisphere by fibres from the ipsilateral inferior olive following unilateral neonatal pedunculotomy: an autoradiographic and retrograde fluorescent double-labelling study. *Exp Brain Res* 62:411–421.
- Shinoda Y, Yokota J, Futami T. 1981. Divergent projection of individual corticospinal axons to motoneurons of multiple muscles in the monkey. *Neurosci Lett* 23:7–12.
- Shinoda Y, Ohgaki T, Futami T. 1986. The morphology of single lateral vestibulospinal tract axons in the lower cervical spinal cord of the cat. *J Comp Neurol* 249:226–241.
- Shinoda Y, Sugiuchi Y, Futami T. 1987. Excitatory inputs to cerebellar dentate nucleus neurons from the cerebral cortex in the cat. *Exp Brain Res* 67:299–315.
- Shinoda Y, Sugiuchi Y, Futami T, Izawa R. 1992. Axon collaterals of mossy fibers from the pontine nucleus in the cerebellar dentate nucleus. *J Neurophysiol* 67:547–560.
- Sugihara I, Lang EJ, Llinás R. 1993. Uniform olivocerebellar conduction time underlies Purkinje cell complex spike synchronicity in the rat cerebellum. *J Physiol [Lond]* 470:243–271.
- Sugihara I, Lang EJ, Llinás R. 1995. Serotonin modulation of inferior olivary oscillations and synchronicity: a multiple-electrode study in the rat cerebellum. *Eur J Neurosci* 7:521–534.
- Sugihara I, Wu H, Shinoda Y. 1996. Morphology of axon collaterals of single climbing fibers in the deep cerebellar nuclei of the rat. *Neurosci Lett* 217:33–36.
- Szentágothai J, Rajkovits K. 1959. Über den Ursprung der Kletterfasern des Kleinhirns. *Z Anat Entwicklungsgesch* 121:130–141.
- Van der Want JJJ, Voogd J. 1987. Ultrastructural identification and localization of climbing fiber terminals in the fastigial nucleus of the cat. *J Comp Neurol* 258:81–90.
- Van der Want JJJ, Wiklund L, Guegan M, Ruigrok T, Voogd J. 1989. Anterograde tracing of the rat olivocerebellar system with *Phaseolus vulgaris* leucoagglutinin (PHA-L). Demonstration of climbing fiber collateral innervation of the cerebellar nuclei. *J Comp Neurol* 288:1–18.
- Veenman CL, Reiner A, Honig MG. 1992. Biotinylated dextran amine as an anterograde tracer for single- and double-labeling studies. *J Neurosci Methods* 41:239–254.
- Voogd J. 1995. Cerebellum. In: Paxinos G, editor. *The rat nervous system*, 2nd ed. San Diego: Academic Press. p 309–350.
- Voogd J, Bigaré F. 1980. Topographical distribution of olivary and cortico nuclear fibers in the cerebellum: a review. In: Courville J, de Montigny C, Lamarre Y, editors. *The inferior olivary nucleus. Anatomy and physiology*. New York: Raven Press. p 207–234.
- Voogd J, Jaarsma D, Marani E. 1996. The cerebellum, chemoarchitecture and anatomy. In: Swanson LW, Björklund A, Hökfelt T, editors. *Integrated systems of the CNS, Part III. cerebellum, basal ganglia, olfactory system*. Handbook of Chemical Neuroanatomy, vol 12. Amsterdam: Elsevier. p 1–369.
- Wiklund L, Toggenburger G, Cuénod M. 1984. Selective retrograde labelling of the rat olivocerebellar climbing fiber system with D-[³H]aspartate. *Neuroscience* 13:441–468.
- Yamamoto T, Fukuda M, Llinás R. 1986. Bilateral synchronization of climbing fiber activity. *Soc Neurosci Abstr* 12:577.